Ore Geology Reviews 72 (2015) 128–148

Contents lists available at ScienceDirect

Ore Geology Reviews

journal homepage: www.elsevier.com/locate/oregeorev

Effects of hydrous alteration on the distribution of base metals and platinum group elements within the Kevitsa magmatic nickel sulphide deposit

Margaux Le Vaillant [a,b,*], Stephen J. Barnes [b], Marco L. Fiorentini [a], Frank Santaguida [c], Tuomo Törmänen [d]

[a] Centre for Exploration Targeting, School of Earth and Environment, Australian Research Council Centre of Excellence for Core to Crust Fluid Systems, The University of Western Australia, Perth, Australia
[b] CSIRO/Minerals Resources Flagship, Perth, Australia
[c] First Quantum Minerals Ltd, FQM FinnEx Oy, 99600 Sodankylä, Finland
[d] Geological Survey of Finland (GTK), FI-96101 Rovaniemi, Finland

ARTICLE INFO

Article history:
Received 23 December 2014
Received in revised form 29 May 2015
Accepted 4 June 2015
Available online 8 July 2015

Keywords:
Ni–Cu–(PGE) deposit
Layered intrusion
Hydrothermal alteration
Base metals and PGE mobility and remobilisation
Paleoproterozoic
Finland

ABSTRACT

Platinum and nickel are commonly assumed to be immobile in most conditions, especially during low temperature hydrothermal alteration. However, only a small number of studies have rigorously tested this assumption. The Ni–Cu–(PGE) sulphide ore body hosted by the Kevitsa intrusion, northern Finland, provides a natural laboratory to study the behaviour of base metals and platinum group elements (PGE) during low temperature alteration. This ca. 2060 Ma mafic–ultramafic intrusion, located in the Central Lapland greenstone belt, hosts disseminated Ni–Cu–(PGE) sulphide mineralisation in the middle part of the main ultramafic body. The mineralisation, which contains a range of Ni, Cu and PGE grades, is affected by three main alterations (serpentinisation, amphibolitisation and epidotisation), and is cross cut by various types of veins. The effect of the circulation of hydrothermal fluids on the distribution of base metals and PGE was studied at two different scales. Interrogation of an extensive deposit-wide assay database provided information on the deposit-scale (kilometre scale) effect of these different alteration styles, and a detailed study, involving laboratory X-ray fluorescence (XRF), portable XRF and micro-XRF mapping, of drill-core samples containing cm-scale cross-cutting veins provided information on the small scale (centimetre to decimetre scale) remobilisation of base metals and PGEs. Results show that the hydration and carbonation of the Kevitsa mineralised mafic–ultramafic intrusion did not significantly affect the distribution of Ni and PGE at scales larger than a few mm, and that Cu and Au are the only metals that are affected by small to large scale remobilisation from centimetre to kilometre scale.

1. Introduction

Platinum group elements (PGEs) are widely used as petrogenetic indicators in ore deposits and their host rocks. Commonly these ores and rocks have been subjected to hydrothermal alteration, particularly in the case of Precambrian terranes and greenstone belts. It is a common assumption that PGEs and nickel are relatively immobile elements, not easily remobilised by hydrothermal fluids, and this assumption underpins their use in petrogenetic interpretations. However, there is good evidence for mobility of PGE and Ni under some circumstances. The conditions favourable for hydrothermal modification of originally magmatic abundances of Ni and PGEs are poorly known, and very few studies to date have systematically examined their mobility. This study aims to address that deficit by investigating distributions of these elements in fresh and altered rocks from a well-characterised, texturally homogeneous disseminated sulphide orebody that has undergone a variety of styles of localised alteration.

Nickel is known to be among the least soluble first-row transition metal in most common geological fluids (Liu et al., 2012). Likewise the platinum group elements are known to have very low solubilities in association with common ligands. Reviewing the extensive literature on PGE solubility in aqueous fluids (e.g. Gammons, 1995, 1996; Mountain and Wood, 1988), Barnes and Liu (2012) concluded that Pt and Pd could readily be soluble as bisulphide complexes in acidic fluids and reduced conditions, and as chloride complexes in unusually acidic and oxidised conditions, accounting for the dispersion and concentration of Pt and Pd in some specific hydrothermal environments. Based on ab initio molecular dynamic modelling backed up by experiments, Mei et al. (2015) showed that Pd is mainly carried as the Pd(HS)$_4^{2-}$ hydrosulfide complex at neutral-alkaline and reduced (pyrite/pyrrhotite stable) conditions, and as the PdCl$_4^{2-}$ chloride complex at

---

* Corresponding author at: Centre for Exploration Targeting, School of Earth and Environment, Australian Research Council Centre of Excellence for Core to Crust Fluid Systems, The University of Western Australia, Perth, Australia.
E-mail address: margaux.levaillant@csiro.au (M. Le Vaillant).

http://dx.doi.org/10.1016/j.oregeorev.2015.06.002
0169-1368/© 2015 Elsevier B.V. All rights reserved.

acidic and oxidised conditions. At 300 °C, significant Pd mobility at ppb level as Pd bisulfide complexes is predicted under fluid-buffered conditions (e.g., pH ~ 7–8, near HS-/H_2S(aq) pH buffer), but only limited Pd solubility is predicted under rock-buffered conditions (e.g., pH ~4–5, quartz–feldspar–muscovite buffer).

Many examples show the importance of hydrothermal remobilisation during the modification or the genesis of Ni–Cu and/or PGE rich ore. Evidence for variations in metal distribution and tenors due to hydrothermal remobilisation has been documented at the Donaldson West Deposit in Québec (Dillon-Leitch et al., 1986), at various locations within the Sudbury Igneous Complex in Canada, such as the Fraser mine, the Barnet property, the Strathcona mine and the McCreedy West mine (Farrow and Watkinson, 1997), at Ni sulphide deposits around the Kambalda Dome in Western Australia (Heath et al., 2001; Lesher and Keays, 1984) and at the Jinbaoshan Pd–Pt deposit in South West China (Wang et al., 2008). Gal et al. (2011) describe PGE minerals associated with the products of Cl-rich late magmatic or hydrothermal fluids in contact rocks of the Duluth Complex, although no whole-rock concentrations were reported. Several PGE-rich ores of hydrothermal origin have also been described over the years, such as the PGE-rich ore formed within cross-cutting faults at the Fortaleza de Minas deposit in Brazil (De Almeida et al., 2007), the low-S Cu–Ni–PGE footwall ores at Sudbury in Canada (Farrow and Watkinson, 1997; Hanley and Mungall, 2003; Molnár et al., 2001a, 2001b; Molnár and Watkinson, 2001), the McBratney deposit in Canada (Bursztyn and Olivo, 2010), and the high Pt concentrations observed in dunite pipes in the Bushveld Complex which are generally regarded as being hydrothermal in origin (Schiffries, 1976). Elevated Pt and Pd contents are found in some porphyry Cu–Au systems (Augé et al., 2005; Economou-Eliopoulos, 1991; LeFort et al., 2011) and unconformity-type uranium deposits (Jaireth, 1992; Mernagh et al., 1994). Finally, several nickel deposits such as the Avebury deposit in Tasmania (Keays and Jowitt, 2013), the Epoch deposit in Zimbabwe (Pirajno and González-Álvarez, 2013), the Doriri Creek deposit in Papua New Guinea (González-Álvarez et al., 2013) and the Enterprise sediment-hosted Ni deposit in Zambia (Capistrant et al., 2015) have been interpreted as having a hydrothermal origin.

Given the wide range of examples of hydrothermal remobilisation of Ni and PGEs, it is necessary to critically examine the common assumption that these elements can be reliably used as alteration-stable trace elements in petrogenetic studies of hydrothermally altered rocks. Barnes and Liu (2012) made a case for relative immobility of PGEs during serpentinisation and talc carbonate alteration of ultramafic rocks (komatiites) in Archaean greenstone terranes, but apart from that study no systematic investigations on the scale and the conditions of PGE mobility in altered rocks exist. Our study uses the Kevitsa Ni–Cu–PGE ore deposit, Finland, as a natural laboratory to test the behaviour of base metals and PGEs during vein-related hydrothermal alteration.

The Kevitsa mineralised ultramafic intrusion has been the subject of many studies which provide good constraints on its geometry, internal compositional variations in base metals and PGE, intensity and distribution of the various hydrothermal alteration styles, and on the main structures possibly affecting the system (Gervilla and Kojonen, 2002; Grinenko et al., 2003; Hanski et al., 2001; Mutanen, 1997; Mutanen and Huhma, 2001; Standing et al., 2009; Yang et al., 2013; Santaguida et al., 2015). The Kevitsa deposit shows a wide range of primary metal tenors, in texturally homogeneous disseminated ores, with rock types ranging from essentially fresh igneous pyroxenites and peridotites to extensively hydrated amphibolites showing a range of different alteration assemblages (Mutanen, 1997). Hence, this deposit is perfect to study the effects of hydrothermal alteration on metal tenors and grades of the sulphides. Our work also addresses specific claims made in previous work (Mutanen, 1997; Standing et al., 2009) that alteration has resulted in significant modification of sulphide and metal concentrations.

2. Geological background

The ca. 2.06 Ga Kevitsa intrusion (Mutanen, 1997; Mutanen and Huhma, 2001) is located in the Central Lapland greenstone belt in northern Finland (Fig. 1A). It is part of a suite of small- to medium-sized mafic–ultramafic intrusions occurring in the area, including the large ca. 2.44 Ga Koitelainen layered intrusion (Mutanen, 1997) as well as the neighbouring Sakatti intrusion hosting the Sakatti Cu–Ni deposit (Coppard et al., 2013), which has not yet been dated.

The Central Lapland greenstone belt, which spans a range of ages from ~2400 Ma to ~1800 Ma, is mainly composed of volcanic rocks ranging from komatiites (Hanski et al., 2001; Heggie et al., 2013) to rhyolites, intercalated with thick sequences of quartzitic to pelitic sedimentary rocks (Hanski and Huhma, 2005; Lehtonen et al., 1998). The Kevitsa intrusion was emplaced into mica schists and black schists of the Matarakoski Formation and is thought to be roughly contemporaneous with komatiitic volcanic rocks (ca. 2.06 Ga; Hanski et al., 2001) which occur in the vicinity of the intrusion (Fig. 1). The Kevitsa intrusion occupies a surface area of approximately 16 km^2 and consists of a lower ultramafic unit up to 2 km in thickness, overlain in an uncertain

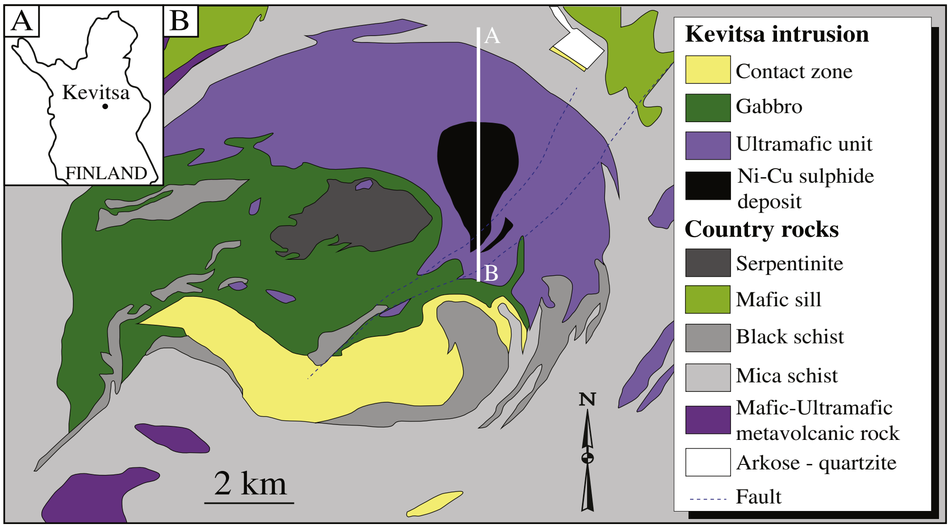

Fig. 1. A) Location of the Kevitsa intrusion in the Central Lapland greenstone belt, northern Finland (after Hanski et al., 2001). B) Simplified geological map of the Kevitsa intrusion (after Mutanen, 1997). Section A–B is presented in Fig. 2.

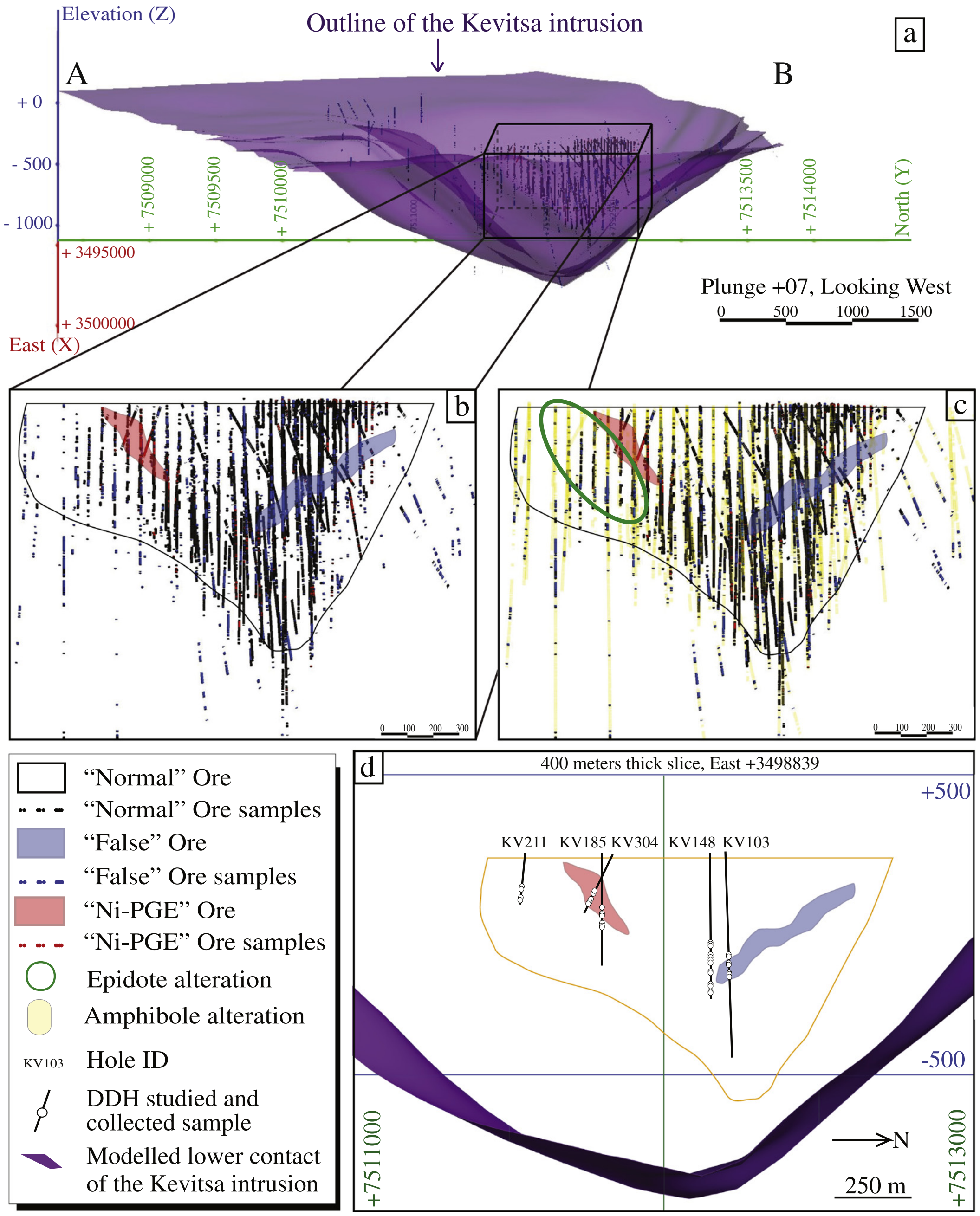

Fig. 2. Geometry of the Kevitsa intrusion based on drill hole intersects, surface mapping and seismic data interpretation, and 3D visualisation of the large scale mine assay database. a) 3D model of the contact between the Kevitsa intrusion and the country rocks and location of the Kevitsa ore body composed of disseminated sulphides. Each dot represents a sample from the mine assay database; b, c) drilling profiles of the ore body indicating the distribution of the different ore types and alteration types (epidote and amphibole rich alterations). d) Cross section through the Kevitsa intrusion with the location of collected samples for the small scale study, using samples containing cross-cutting veins.

relationship by a gabbro unit over several hundred metres thick (Fig. 1B). The ultramafic unit is composed of interlayered olivine pyroxenite and websterite, with a local development of cyclic units, but for the most part lacking obvious internal layering. The upper portion of the ultramafic unit contains abundant xenoliths of ultramafic rocks, whereas pelitic xenoliths become more abundant towards the base of the intrusion (Gervilla and Kojonen, 2002). The gabbroic unit is made up of gabbro, ferrogabbro, and magnetite gabbro (Mutanen, 1997).

The Kevitsa Ni–Cu–(PGE) deposit, also referred to in the literature as the Kevitsansarvi deposit (Gervilla and Kojonen, 2002), occurs in the middle part of the ultramafic unit, associated with variably layered olivine pyroxenites and websterites. The deposit consists entirely of disseminated sulphides with varying Ni, Cu and PGE tenors. Low tenor ores form near the base of the intrusion and along the margins of the Cu–Ni mineralisation. Two main types of ore are distinguished within the ore body, largely on the basis of Ni and PGE tenors. These are referred to as "normal" (or Cu–Ni) type and Ni–PGE type (Fig. 1). The normal ore type occurs as a series of continuous bodies that may extend for hundreds of metres and represent the bulk (>90%) of the economic resource. The normal ore is characterised by 2–6 vol.% of sulphides (pyrrhotite, pentlandite, and chalcopyrite) and average Ni and Cu ore-grades of 0.3 and 0.4 wt.%, respectively. The Ni–PGE ore occurs locally both in the upper and lower part of the mineralised zone as small, discontinuous lens-like bodies ranging from several metres to tens of metres in thickness. The Ni–PGE ore has a similar sulphide content to that of the normal ore, but the sulphides are predominantly pentlandite, pyrite and millerite, and the ores have higher and more variable Ni grades, lower Cu grades (Ni/Cu = 1.5–15) and extreme Ni tenors in excess of

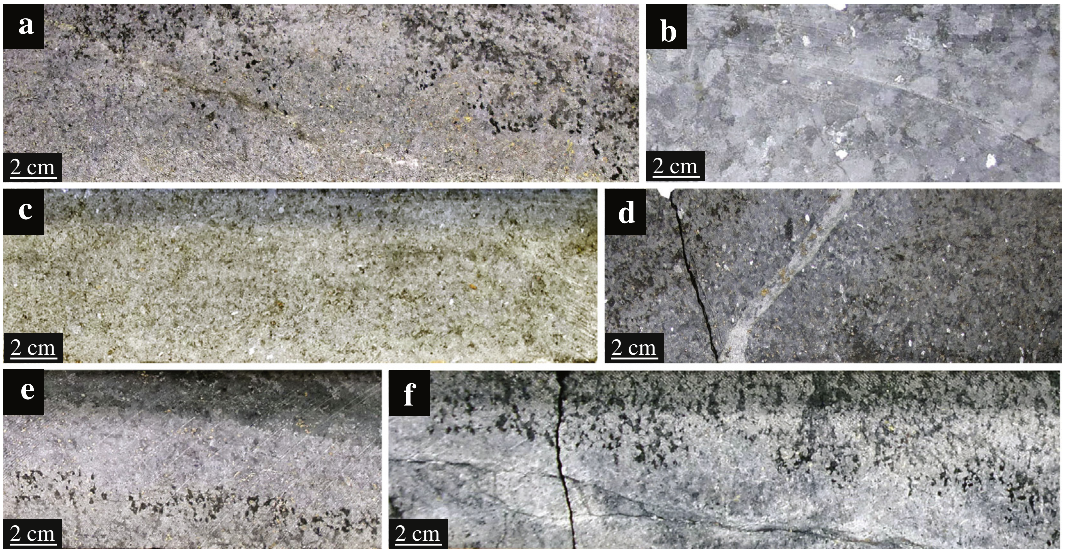

Fig. 3. Drill core photos of the various alteration types and vein types observed within the Kevitsa intrusion and studied during this project. a) Patchy amphibole alteration, sample KV148-474; b) thin quartz-carbonate vein and associated amphibole rich alteration, sample KV304-157.1; c) epidote rich alteration, KV304-142.7; d) thick carbonate vein with an important amphibole rich selvedge, Sample KV103-407.2; e) actinolite–chlorite–epidote rich vein and associated amphibole-rich selvedge, sample KV103-438.4; and f) thin carbonate vein with amphibole rich associated selvedge, sample KV148-305.5.

30%. Extremely high Ni contents are also observed in primary silicates in the Ni–PGE ore type (Yang et al., 2013). It is likely that these Ni–PGE ores constitute another example of extremely high Ni tenor ores related to the formation from Ni-enriched magmas at high values of silicate to sulphide mass ratio (R factor) in the presence of olivine (e.g. Barnes et al., 2013). Pyrrhotite-rich mineralisation associated with country rock xenoliths, dominantly disseminated but locally net-textured and semi-massive at the decimetre scale, is widespread through the intrusion outside the main ore body, and is referred to as “false ore” by the mine geologists.

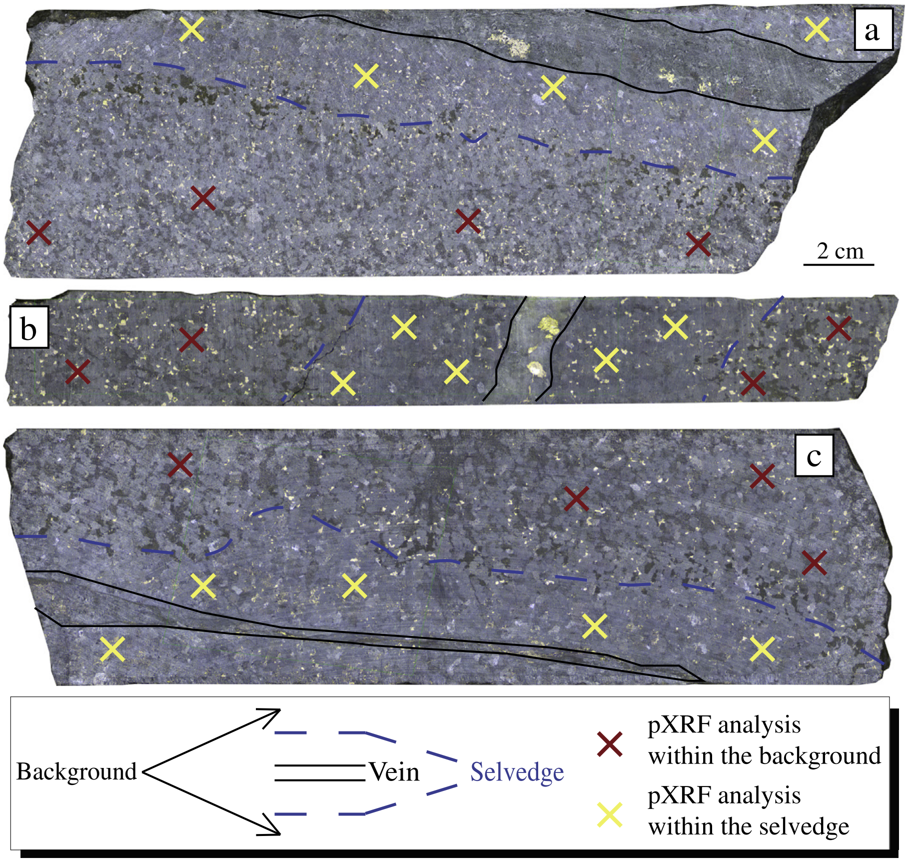

Fig. 4. Schematic representation of the methodology used to evaluate the sample precision (representing the sample heterogeneity) and to evaluate element fluxes between background and altered (selvedge) areas of the samples collected for the detailed-scale study using portable XRF. a) Actinolite–chlorite–epidote vein, sample KV103-438.4, b) Thick carbonated vein, sample KV103-407.2, c) Thin carbonate vein, sample KV148-305.5.

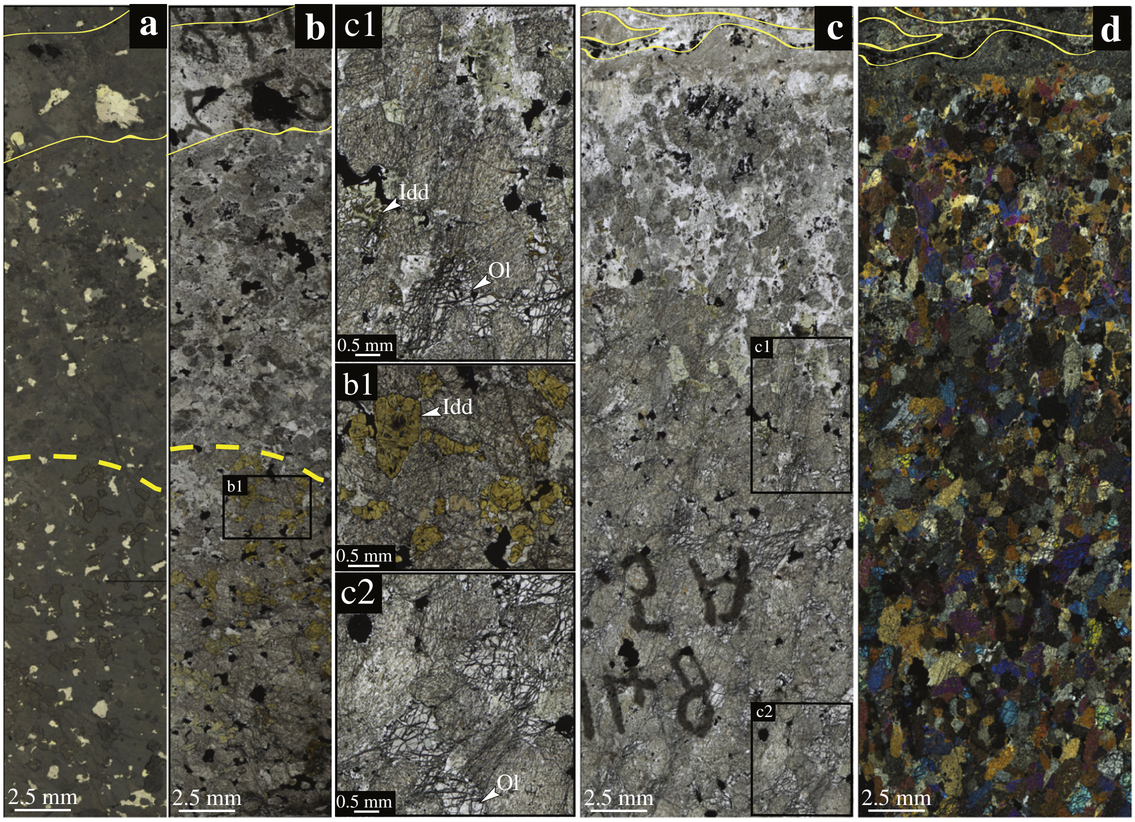

Fig. 5. Photomicrographs of thin sections of samples cross cut by carbonate veins. a and b are photomicrographs of the whole length of the thin section of sample KV103-407.2 in reflected (a) and transmitted light (b). c and d are photomicrographs of the whole length of the thin section of sample KV148-305.5, in transmitted (c) and cross polarised light (d). b1, c1 and c2 are close up photomicrographs of both samples in transmitted light, showing the progressive alteration of olivine into iddingsite, and then total replacement by a fine grain mixture of quartz and chlorite in the close selvedge of the vein. In c and d, the darker shapes are due to the names of the samples which have been engraved in the back of the glass slice.

The greenstone sequence and the Kevitsa intrusion were metamorphosed and hydrothermally altered during regional greenschist facies metamorphism (Mutanen, 1997), producing various alteration zones and cross-cutting veins. The Kevitsa intrusion has been interpreted by Mutanen (1997) as a sequence of olivine–clinopyroxene–orthopyroxene–magnetite cumulates with intercumulus minerals including plagioclase, biotite–phlogopite, brown hornblende, Cl-rich amphibole, chlorapatite, monazite, graphite, and ilmenite. Sulphides occur as interstitial aggregates of cumulus origin, comprising pyrrhotite, chalcopyrite and pentlandite with minor low-temperature cubanite and makinawite. During metamorphism and retrograde processes, primary magmatic minerals were partially hydrated to serpentine, amphiboles, talc, chlorite and phlogopite, whereas intercumulus plagioclase grains were altered to chlorite, clinozoisite–epidote, carbonate and scapolite (Mutanen, 1997). Extensive hydrothermal alteration is mainly concentrated in the southern part of the intrusion, whereas igneous rocks in the northern part of the intrusion are largely fresh. Multiple sets of quartz-carbonate veins and actinolite–chlorite–epidote veins occur throughout the deposit. The orientation and distribution of these vein sets are poorly constrained from diamond drilling, but recent mining has revealed some preferred trends which are the focus of future work.

3. Materials and methods

In this study, we took a multi-scale approach to assess the extent and nature of metal redistribution through hydrothermal processes.

(1) Deposit scale study: two large databases were interrogated: the First Quantum Minerals Ltd (FQM) resource drilling assay database (encompassing over 20 years of diamond drilling and exploration, 1992–2012), and a vast PGE analytical database of nearly 10,000 6-element PGE analyses from the Geological Survey of Finland, GTK (Mutanen, 1997). In order to assess any statistically significant difference between fresh and altered rocks, these datasets were combined with mine-site logging codes reporting alteration style and intensity, and variations in metal tenors and grades.

(2) Detailed-scale study: veins that are cross-cutting otherwise homogeneous portions of the ore body were sampled in order to determine if any consistent metal addition or loss signatures could be detected in and out of vein selvedges. Veins were sampled to be representative of the range of different alteration styles. Our study involved portable X-Ray Fluorescence (pXRF) measurements, whole-rock laboratory measurements on major, trace elements and PGEs in vein selvedges and adjacent fresh rock, element mapping at hand sample scale using a desktop microbeam XRF mapping instrument, and petrographic study. Results are reported using a variation of the “isocon” mass balance approach estimating element fluxes in metasomatic environments (Grant, 1986; Gresens, 1967; Gresham, 1986).

3.1. Deposit-scale study

Two large datasets were used in this deposit-scale (km) study: the resource drilling assay database (as of March 2012) and the vast PGE analytical database from the Geological Survey of Finland (GTK) (reported in Mutanen, 1997 and example for drill hole R326 shown in the Supplementary material Table 7). Samples analysed within these datasets give a very good spatial representation of the Kevitsa ore body (Fig. 2). The

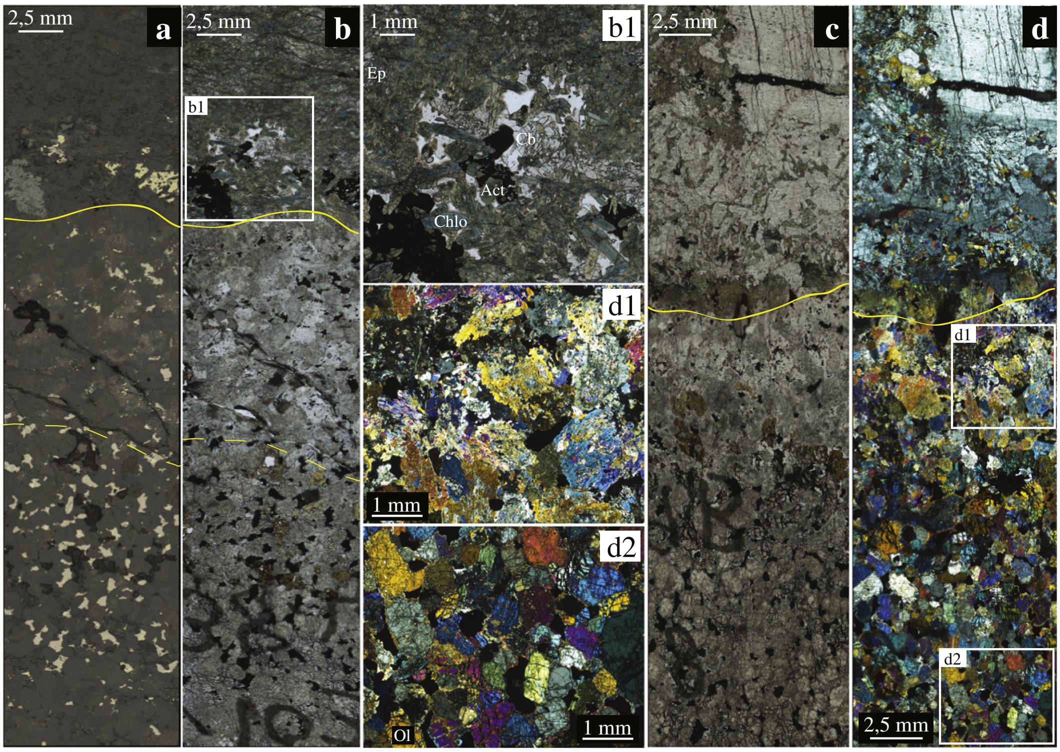

Fig. 6. Photomicrographs of thin sections of samples KV148-339.9 and KV103-438.4 cross cut by actinolite–chlorite–epidote ± albite veins. a and b are photomicrographs of the whole length of the thin section of sample KV103-438.4 in reflected (a) and transmitted light (b), c and d are photomicrographs of the whole length of the thin section of sample KV148-339.9, in transmitted (c) and cross polarised light (d). b1, d1 and d2 are close up photomicrographs in transmitted (b1) and cross polarised light (d1 and d2). Photomicrograph (b1) illustrates the characteristic composition of actinolite–chlorite–epidote veins. Photomigrograph (d1) illustrates the typical alteration observed in close proximity to the veins, and photomicrograph (d2) illustrates the typical background composition. In b, c and d, the darker shapes are due to the names of the samples which have been engraved in the back of the glass slice.

database provides concentrations in Ni, NiS (nickel in sulphides), Cu, Co, S, Au, Pd, and Pt for 26,099 samples, and out of these, 9244 have also been analysed by the Geological Survey of Finland (GTK) for the full suite of PGE (Pd, Pt, Rh, Ru, Os and Ir) and Au. These 26,099 samples are spread over the mineralised area of the intrusion and comprise samples of normal, Ni–PGE, and false ore. The resource drilling assay database is composed of three different drilling campaigns which are described in details in technical report 43-101 from First Quantum

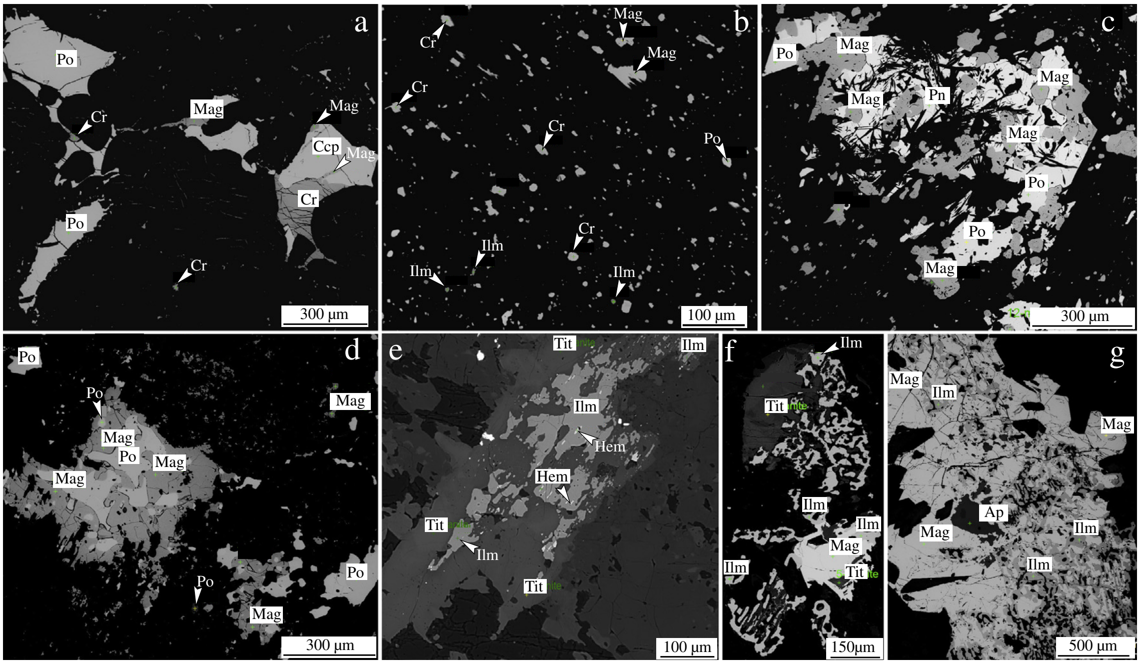

Fig. 7. SEM EDS photomicrographs of oxide assemblages within the background, selvedge areas and cross-cutting veins. Background composition is represented by photomicrograph a) of sample KV103-407.2, textures and assemblages observed within the selvedge area are illustrated by photomicrographs b, c and d (samples KV103-407.2, KV148-305.5 and KV103-438.4) and textural relationship and mineralogical assemblages of oxides in all the different types of veins are illustrated in photomicrographs e, f and g (samples KV148-339.9 and KV103-438.4). Abbreviations: Po pyrrhotite, Ccp chalcopyrite, Pn pentlandite, Mag magnetite, Ilm ilmenite, Hem haematite, Tit titanite, Cr chromite, Ap apatite.

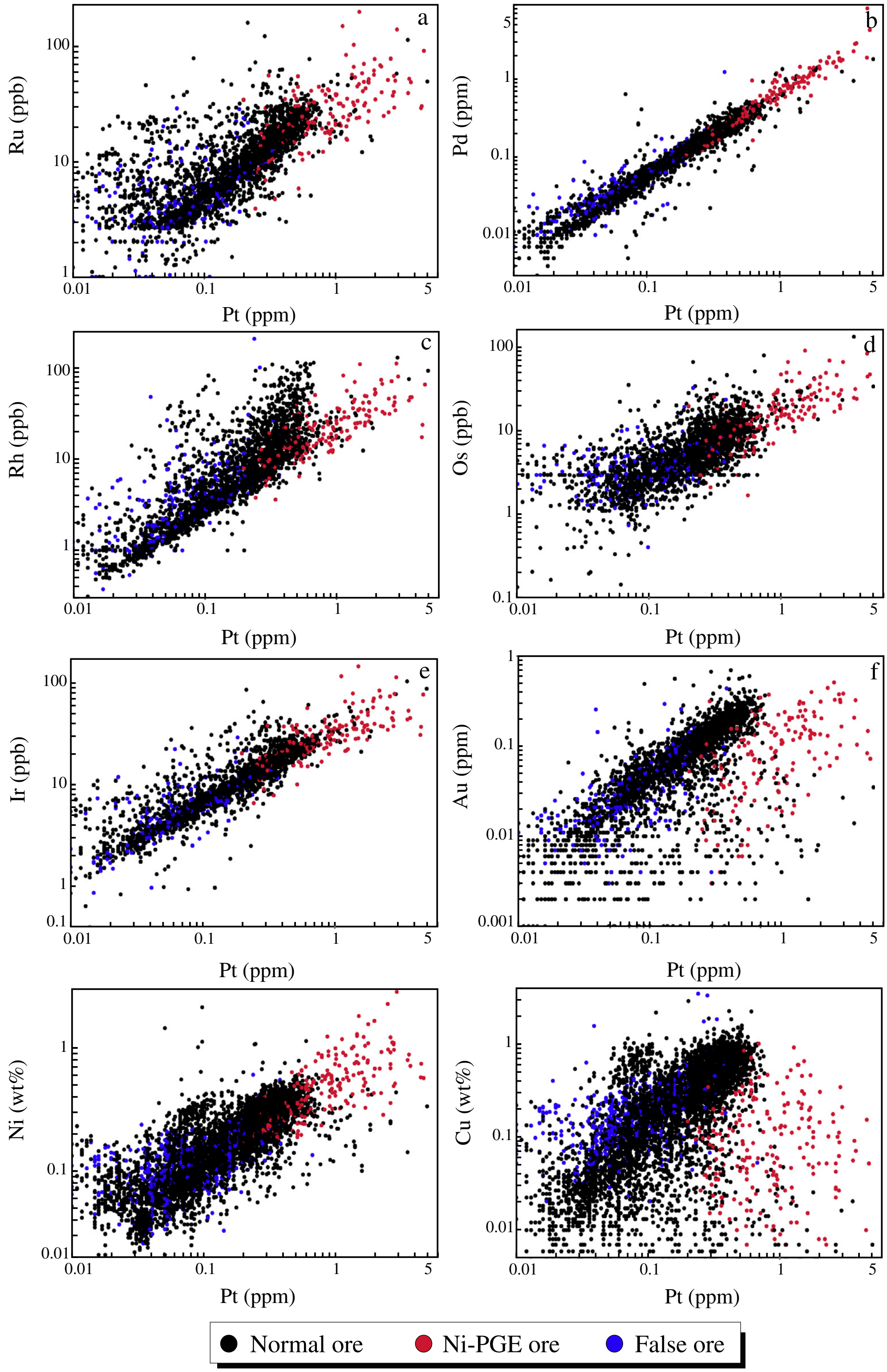

Fig. 8. Variations of PGE concentrations in different ore types of the Kevitsa ore body. Data from the Geological Survey of Finland's database (GTK) (9244 analyses).

Minerals Ltd (FQM) (Gregory, 2011), as well as in the Supplementary materials.

Three main alteration styles have been logged in the database with 5,321 amphibole-altered samples, 184 serpentinite-altered samples, and 61 epidote-altered samples. The approach used was to compare inter-element correlation patterns between Ni, Cu, Co, S and PGE for fresh samples, and samples representing the two main alteration styles, identified during the initial logging of the drill core by mine geological staff. Due to the prolonged period of drilling, and the fact that multiple companies with different geologists and logging systems operated, some classifications uncertainties exist due to inconsistency in terminologies and identifications. However, given the very large size of the

Table 1
Correlation coefficients between the various PGE using the GTK assay database (9244 samples). Colour codes: white = 0 < R < 0.5; yellow = 0.5 < R < 0.7; red = 0.7 < R < 1.

GTK database – 9244 samples

	Pd	Pt	Ir	Ru	Rh	Os	Ni	Cu	Au
Pd	1	0.93	0.7	0.59	0.48	0.6	0.62	0.18	0.31
Pt	0.93	1	0.8	0.66	0.55	0.68	0.66	0.22	0.35
Ir	0.7	0.8	1	0.9	0.63	0.8	0.69	0.29	0.38
Ru	0.59	0.66	0.9	1	0.59	0.74	0.62	0.28	0.36
Rh	0.48	0.55	0.63	0.59	1	0.49	0.59	0.53	0.5
Os	0.6	0.68	0.8	0.74	0.49	1	0.56	0.25	0.31
Ni	0.62	0.66	0.69	0.62	0.59	0.56	1	0.59	0.52
Cu	0.18	0.22	0.29	0.28	0.53	0.25	0.59	1	0.59
Au	0.31	0.35	0.38	0.36	0.5	0.31	0.52	0.59	1

data set, and the distinctive appearance of extensively amphibolitised and epidotised material relative to fresh ultramafic rock (Fig. 3), this approach is unlikely to contain any substantial sampling bias. Moreover, re-logging of drill core sampled in this study, as well as subsequent campaigns, have verified the general distinction between fresh and intensely altered rocks.

3.2. Detailed-scale study

Representative samples of two vein types (quartz-carbonate and actinolite–chlorite–epidote veins) were collected. Twenty samples containing cross-cutting veins with visible selvedge were selected for the study. The location of these samples within the Kevitsa ore body in relation to the various ore types is presented in Fig. 2d. These veins cross cut both the mineralised part of the intrusion (normal ore and Ni–PGE ore), and the barren part. Multiple types of analyses were collected on these samples. The first screening was done by collecting portable XRF (pXRF) analyses on all 20 samples, both in the selvedge of the veins and in the unaltered parts (Fig. 4). Results of these analyses were used to estimate element fluxes by comparing fresh rock compositions with vein selvedge compositions using an isocon plot technique. A subset of 7 samples was studied and imaged in detail using micro-XRF mapping. The same samples were then sent to Geoscience Laboratories in Canada, for precise low-level geochemical analyses to compare with results from portable XRF, and to study the behaviour of platinum group elements using the same isocon technique. The isocon techniques as well as the 'spider' isocon plots are explained and described in details in Supplementary Material.

3.2.1. Portable X-Ray Fluorescence (pXRF) analyses

Our pXRF study followed the analytical protocol described in Le Vaillant et al. (2014). Portable XRF represents an ideal tool to study spatial variations in composition of various elements at a centimetre scale in drill core samples. However, great caution must be taken in the evaluation of the sample precision of the obtained results. Due to the size of the analysing window, pXRF analyses on drill core surfaces (as opposed to finely crushed and pulverised rock) only represent the composition of a 1.5 cm^2 area of the sample, which are generally representative for fine-grained homogeneous samples but may not be for coarser-grained, heterogeneous samples. In the case of the Kevitsa ultramafic intrusion, the sulphide grains are approximately 0.6 mm in diameter in the selvedges of veins and 0.8 mm in diameter in the background area, whereas the average grain size of silicates is approximately

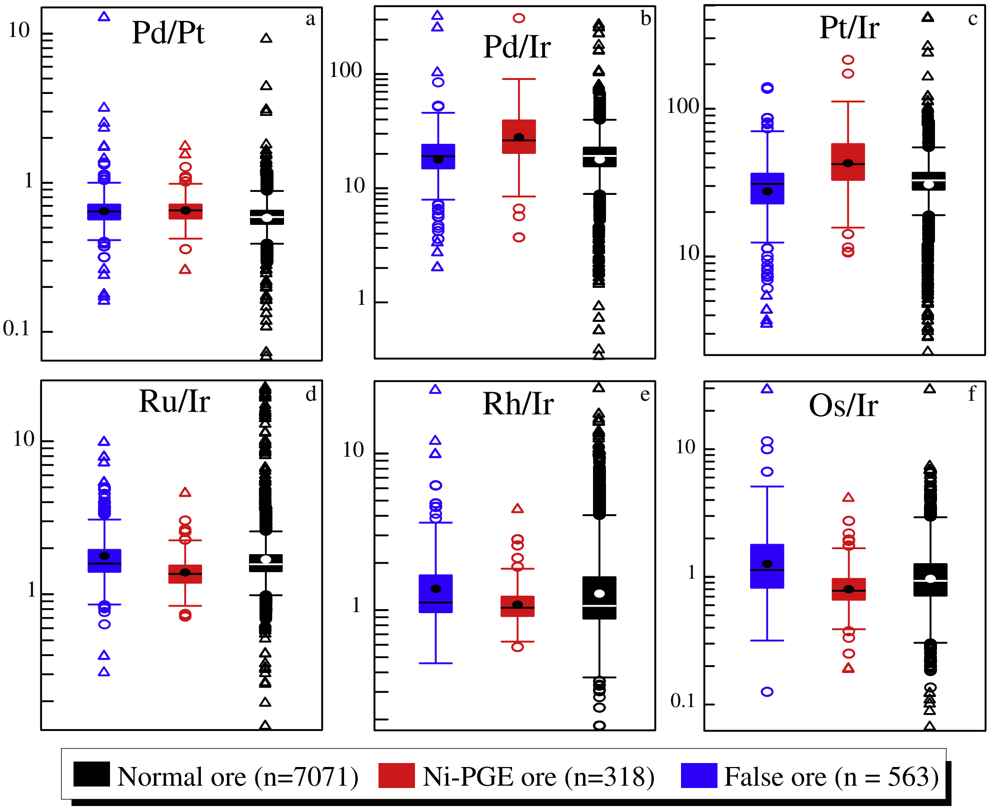

Fig. 9. Comparison of the different PGE ratios for the various ore types using the analytical results from the GTK database (9244 analyses). The central box is the middle 50% of the data from Q1 (bottom of the box which represents the 25th percentile) to Q3 (top of the box which represents the 75th percentile). An outlier (circle) is further than 1.5*(Q3–Q1) from the box. A far outlier (triangle) is further than 3.0*(Q3–Q1) from the box. The whiskers are the extreme values that are not outliers. The line in the middle of the box represents the median and the black dot represents the mean.

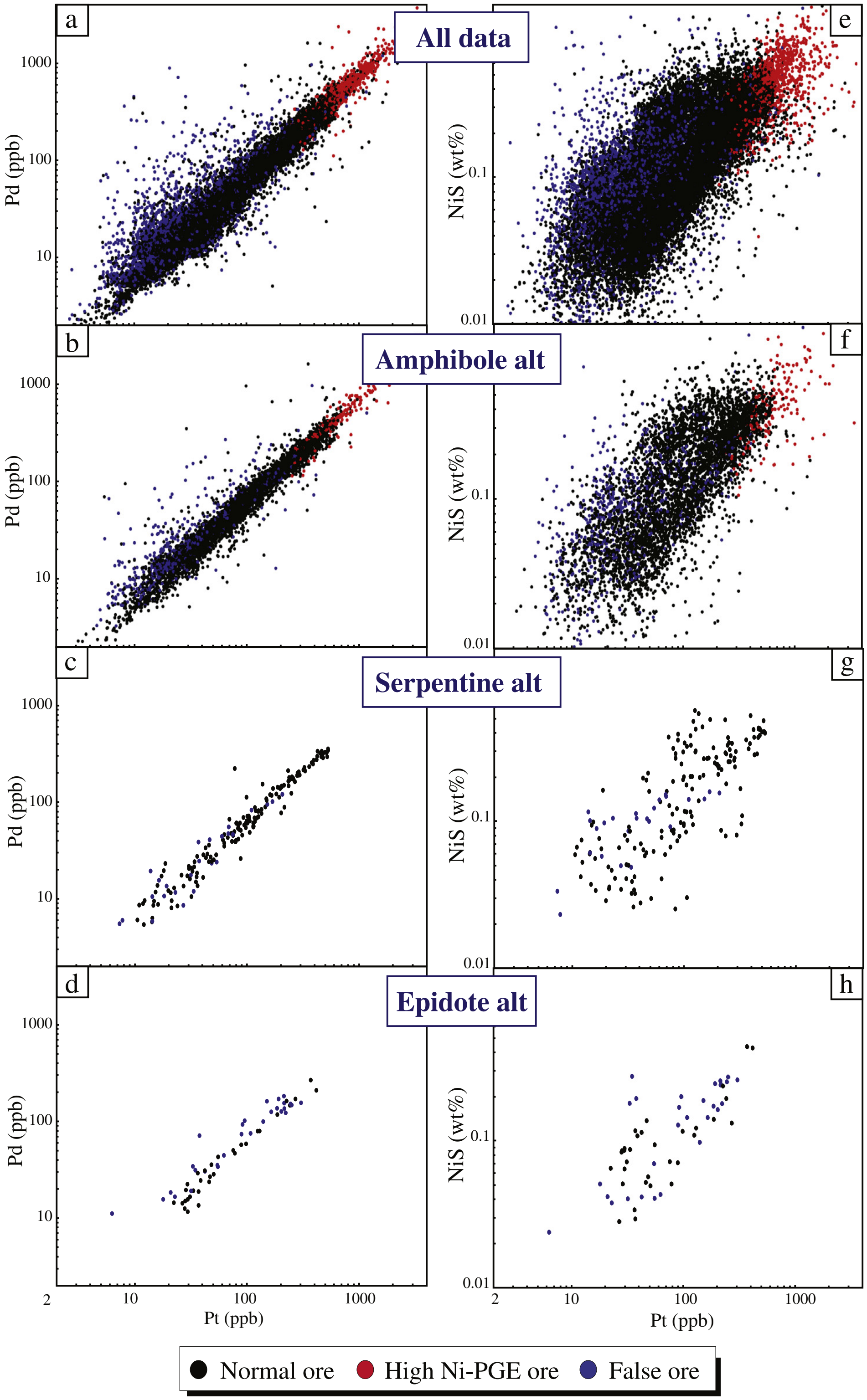

Fig. 10. Pd vs Pt diagrams (a–d) and NiS vs Pt diagrams (e–h) showing variations in the whole dataset and different alteration styles (mine assay database; n = 26,044). NiS = nickel concentration in sulphides, alt = alteration.

1 mm in diameter. Moreover, sulphide aggregates are relatively heterogeneous (pyrrhotite, pentlandite and chalcopyrite mainly). These grain sizes, which are large, combined with the heterogeneity of the composition of the rock, will impact sample precision and the analyses will not be adequately representative of the sample as a whole.

In order to overcome this problem of representativeness of the analyses, the sample precision was thoroughly evaluated (detailed in Supplementary Materials), multiple analyses were performed in order to average the results and the mean of these multiple analyses was used in the isocon study.

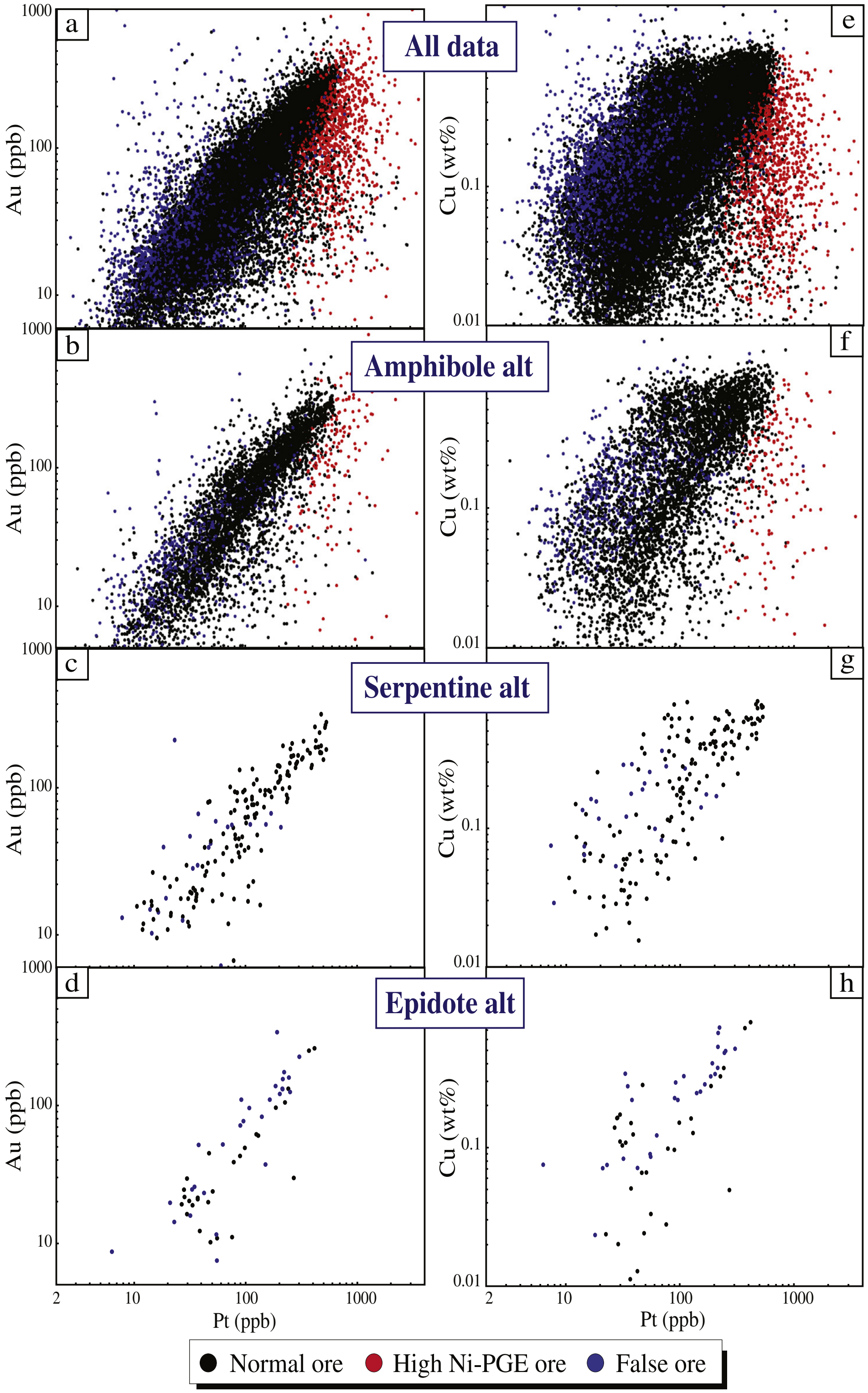

Fig. 11. Cu vs Pt diagrams (a–d) and Au vs Pt diagrams (e–h) showing variations in the whole dataset and different alteration styles (mine assay database; n = 26,044). alt = alteration.

In order to produce spider-isocon plots, 237 pXRF analyses were collected with an Olympus Innov-X Desktop X500 X-Ray fluorescence analyser on coarsely polished half core in both the background area and the altered area (selvedge) of 21 samples with cross-cutting veins (average of 11 analyses per sample, all the results are tabulated in the Supplementary material Table 4). These pXRF analyses gave reliable results for a range of major and trace elements: Ca, K, S, Fe, Ti, Cr, Mn, Ni, Cu, Zn, Zr, Rb and Sr. In order to control the quality of the pXRF data, a comparison study with laboratory data was conducted and is detailed in Supplementary Material.

3.2.2. Laboratory analyses

Seven of the studied "vein" samples were divided into two (background and selvedge, excluding the vein) and sent to the Ontario Geological Survey's Geoscience Laboratories in Sudbury, Canada, for low-level geochemical analyses. Details of the analytical protocol can

Table 2
Correlation coefficients between the various PGE and base metals using the Mine assay database (26,099 samples). Colour codes: white = 0 < R < 0.5; yellow = 0.5 < R < 0.7; red = 0.7 < R < 1.

Mine assay database all – 22,099 samples					
	NiS	Pd	Pt	Au	Cu
NiS	1	0.62	0.65	0.61	0.57
Pd	0.62	1	0.94	0.5	0.24
Pt	0.65	0.94	1	0.57	0.29
Au	0.61	0.5	0.57	1	0.67
Cu	0.57	0.24	0.29	0.67	1
Mine assay database amphibole alteration – 5,321 samples					
	NiS	Pd	Pt	Au	Cu
NiS	1	0.63	0.64	0.62	0.67
Pd	0.63	1	0.94	0.59	0.34
Pt	0.64	0.94	1	0.65	0.38
Au	0.62	0.59	0.65	1	0.72
Cu	0.67	0.34	0.38	0.72	1
Assay database serpentine alteration – 184 samples					
	NiS	Pd	Pt	Au	Cu
NiS	1	0.46	0.35	0.31	0.45
Pd	0.46	1	0.98	0.85	0.64
Pt	0.35	0.98	1	0.89	0.65
Au	0.31	0.85	0.89	1	0.85
Cu	0.45	0.64	0.65	0.85	1
Assay database epidote alteration – 61 samples					
	NiS	Pd	Pt	Au	Cu
NiS	1	0.85	0.83	0.81	0.88
Pd	0.85	1	0.95	0.85	0.79
Pt	0.83		1	0.85	0.82
Au	0.81	0.85	0.85	1	0.86
Cu	0.88	0.79	0.82	0.86	1

be found in Supplementary Materials, and all the results are tabulated in the Supplementary material Table 6.

3.2.3. Element mapping

Five representative samples were mapped using micro-X-Ray Fluorescence (μ-XRF) analysis. This technique allows the production of elemental maps, which can be used to characterise the samples in detail, observe spatial variations, and identify associations among elements. The instrument that was used to collect the data is a Bruker M4 TORNADO™ equipped with a rhodium target X-ray tube operating at 50 kV and 600 nA with a XFlash® silicon drift X-ray detector. Analyses were then quantified using the Bruker ESPRIT software. Maps were created using a 25 μm spot size on a 25 μm raster with dwell times of 10 ms per pixel. Maps are represented as unquantified background-corrected peak height data for Kα peaks for each element. Quantification of areas of the maps was done using the proprietary Bruker M4 EDS X-ray spectrometry software. Spectra for each pixel were combined and averaged over polygonal areas defined graphically on the raw count image, peak heights were determined using a proprietary peak stripping algorithm, basic ZAF corrections applied for a pre-determined range of elements, and results were normalised to 100% on the basis of oxides. The method is semi-quantitative owing to the relatively poor analytical precision for the lighter elements, particularly Na, Mg and Al, but produces highly consistent relative counting statistics for elements heavier than Cl.

4. Results

4.1. Alteration types and veining at Kevitsa

4.1.1. Alteration

The Kevitsa intrusion has undergone multiple types of alteration. The peridotitic rocks are affected by a pervasive, partial serpentinisation of olivine. An epidote (-silica) rich alteration is also observed, structurally controlled and associated with NE-trending faults through the deposit (Fig. 3c). A widespread amphibole rich alteration is observed within the whole intrusion, consisting of progressive epitaxial pseudomorphic replacement of clinopyroxene and orthopyroxene by tremolite–actinolite and cummingtonite–grunerite respectively, producing a pervasive or patchy light green colour (Fig. 3 a,b). Finally, a late stage potassium-rich hydrothermal fluid also circulated through the system producing veinlets and small shear zones enriched in biotite/phlogopite. The predominant alteration styles that can be consistently logged and recognised by the mine-site geologists are the serpentinisation, amphibolitisation and epidotisation. The epidote style (Fig. 3c) is concentrated within specific planar zones towards the south end of the ore body (Fig. 2 c), whereas the amphibole and serpentinite styles are dispersed throughout the intrusion (Fig. 2 c), and enclose decimetre-scale patches of essentially fresh igneous rock. The effect of these three alteration types on the distribution and possible remobilisation of metals and PGE was studied by combining information on their spatial distribution with the results of the deposit-wide resource drilling assay database.

4.1.2. Veining

Multiple veins cross cut the intrusion and different types are observed. Out of these different vein types, two were selected for study.

The most common vein type observed is carbonate (-quartz) veins, commonly associated with a distinctive selvedge, particularly enriched in actinolite and chlorite in close proximity to the vein (Fig. 3d, f and Fig. 5). Amphibole-rich alteration is commonly present in the selvedge of these carbonate veins. Large amphibole alteration zones containing closely spaced carbonate and carbonate-quartz veins are common throughout the intrusion; the veins are intimately associated with the alteration.

The second set of veins used for the study is mainly composed of actinolite partially altered to chlorite, with epidote and minor amounts of carbonates and albite (Figs. 3e and 6). These veins cross cut the Kevitsa deposit in many areas and are almost always associated with a distinct amphibole-rich alteration halo. For the purpose of this detailed study samples were selected that contain cross-cutting actinolite–chlorite–epidote and quartz and/or carbonate veins associated with an alteration selvedge.

4.1.3. Petrographic study

Within the samples used for the small scale study of vein selvedges, four representative samples were selected and studied in detail. Two samples are cross cut by a carbonate vein (KV103-407.2 and KV148-305.5, Fig. 5) and two are cross cut by an actinolite–chlorite–epidote vein (KV148-339.9 and KV103-438.4, Fig. 6). Within these four samples, the mineralogy of the background area is similar, mainly composed of olivine and orthopyroxene with expitaxial replacement by amphiboles (cummingtonite and anthophyllite) (Fig. 6). Interstitial sulphide droplets are primarily composed of pyrrhotite, pentlandite, minor chalcopyrite, chromite and magnetite. In these four different samples, a similar progressive alteration of the olivine grains with proximity to the veins

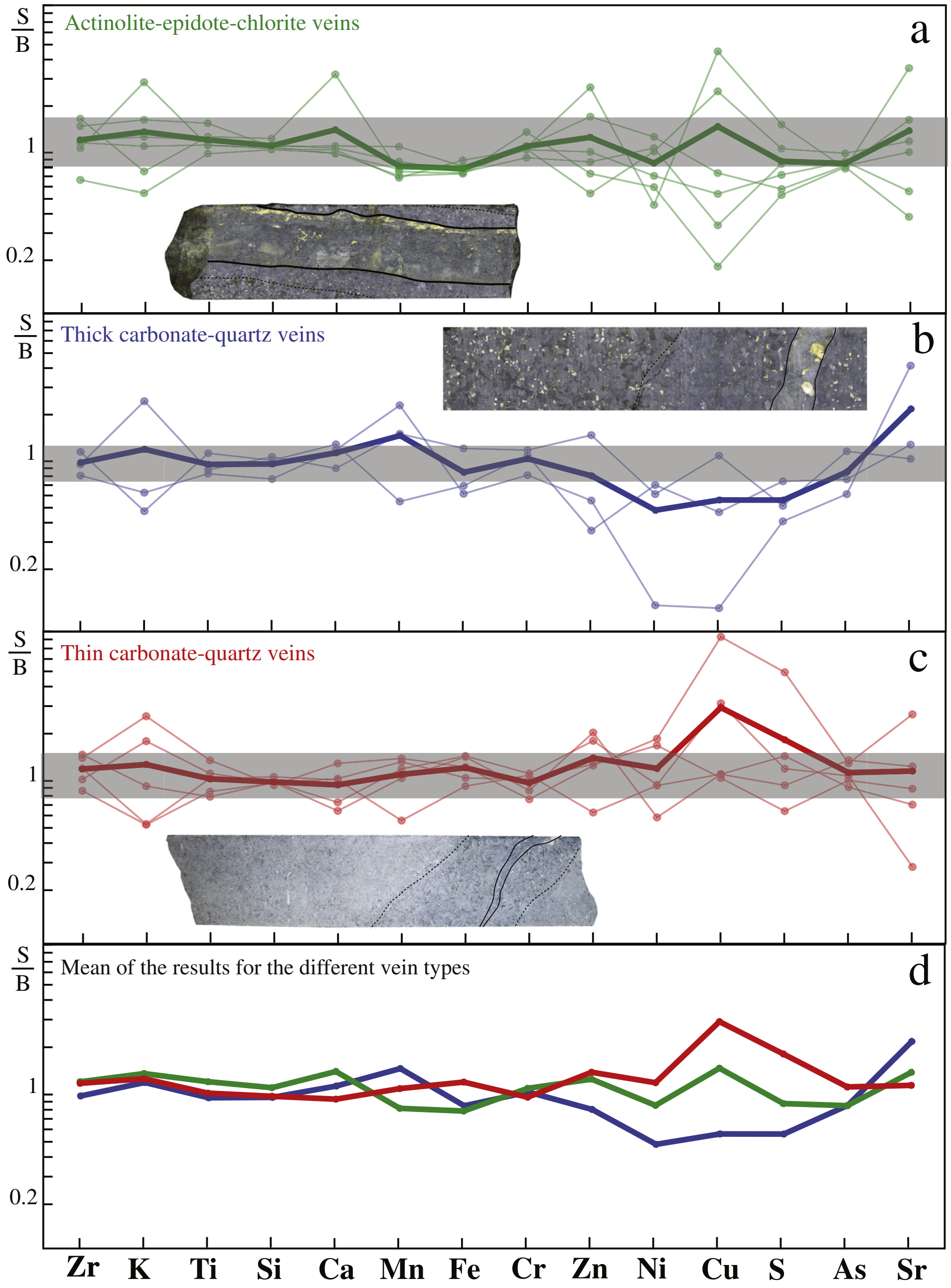

Fig. 12. Spider isocon diagram for pXRF analyses from various samples containing cross-cutting veins with a large selvedge. S/B: Selvedge/Background. In each sections (a, b and c), thin lines represent the mean of multiple analyses collected on one sample. For example, in Fig. 12a there are 6 thin green lines, with each representing the results obtained on 6 different samples averaged to only plot in one line. The thick lines represent the mean of all the results obtained for this vein type. Finally, the thick grey transparent line represents the conserved mass line (isocon). The drill core sample images presented in this figure represent the vein type in general. (For interpretation of the references to colour in this figure legend, the reader is referred to the web version of this article.)

is observed (Fig. 5). Olivine grains are altered to iddingsite (fine grained mixture of clay minerals, iron oxides and ferrihydrites), and completely altered within the close selvedge of the vein. Another common feature is the pervasive amphibole alteration within the selvedge with characteristic replacement of the pyroxenes grains by fine grained actinolite–tremolite assemblages (Fig. 6). Small grains of chlorite and epidote (only in actinolite–chlorite–epidote veins) are dispersed throughout the selvedge. In sample KV148-305.5, a very fine-grained, thin selvedge of actinolite and chlorite is present in close proximity to the vein (Fig. 5c, d). Finally, the sulphides within the selvedge areas are broken down into smaller grains, with an increase in the amount of magnetite, which in places is produced by the oxidation of pyrrhotite grains, and the development of small grains of ilmenite (Fig. 7b, c, d).

Even though the compositions of the selvedges in the various samples are similar, the compositions of the veins vary. In samples KV103-407.2 and KV148-305.5, the carbonate veins contain significant amounts of magnetite, but no other oxides, whereas the actinolite–chlorite–epidote veins in samples KV148-339.9 and KV103-438.4 contain a more complex assemblage of oxides, including magnetite and ilmenite, but also a small amount of titanite and very minor haematite (Fig. 7e, f, g) apparently replacing ilmenite.

4.2. Deposit-scale remobilisation — database study

The study of the composition in PGEs of the Kevitsa intrusion mineralised area (9,244 samples) revealed strikingly strong correlations

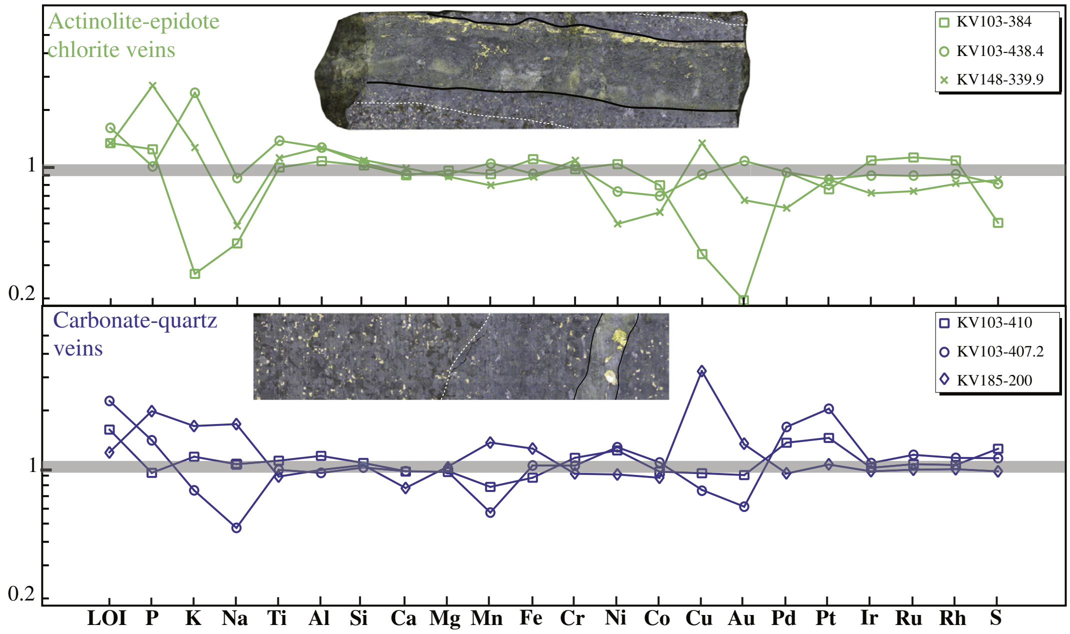

Fig. 13. Spider isocon diagram for laboratory analyses of both altered (selvedge area) and background samples. S/B: Selvedge/Background. The drill core sample images presented in this figure represent the vein type in general.

(Fig. 8). Platinum and Pd are particularly well correlated with a 2:1 ratio ($R = 0.93$, Table 1), and so are Ir and Pt ($R = 0.8$, Table 1). These correlations are observed in all the different ore types (normal ore, Ni–PGE ore and false ore), regardless of their alteration style. Platinum and all the other PGEs are also correlated with nickel (Table 1). Finally, Cu and Au also show a correlation with Pt, but a weaker one especially for "Ni–PGE ores" (Fig. 8), whereas they correlate between each other ($R = 0.59$, Table 1). Correlation coefficients calculated for all the PGE, Ni Cu and Au are tabulated in Table 1.

Finally, in order to evaluate possible decoupling between the PGE, various ratios were studied and compared for the different ore types. Pd/Pt is very similar for the three different ore types, with a median of 0.64 for false ore, 0.59 for normal ore and 0.65 for Ni–PGE ore (Fig. 9). Similarly, ratios between the various IPGE (Iridium-group PGEs) and Ir (Rh/Is, Os/Ir, Ru/Ir) are very similar for the different ore types. However, ratios between IPGE and PPGE (palladium-group PGEs) differ between false ore, normal ore and Ni–PGE ore. The Ni–PGE ore has higher Pd/Ir and Pt/Ir (as well as Pd/Rh, Pt/Rh, Pd/Os, Pt/Os, Pd/Ru and Pt/Ru) than the normal and the false ores (Fig. 9).

The effect of alteration on the strength of correlations between PGE and other chalcophile elements (Cu, Ni, Au) was studied using an even larger dataset (resource drilling assays on 26,099 samples). Three main alteration types, amphibole, serpentine and epidote, were considered. Results show that amphibole altered samples, serpentine altered samples, as well as epidote altered samples conserve the very strong correlation between Pd and Pt (Fig. 10), but also between Ni in sulphides and Pt (Fig. 10), as well as between Cu, Au and Pt (Fig. 11).

Correlation coefficients were calculated between the various PGE and base and precious metals for the whole database and for amphibole-, serpentine- and epidote-altered samples only (tabulated in Table 2). In general, correlations between Ni, Cu, Pd, Pt and Au tend to be even stronger for altered rocks (not depending on the alteration type) than for the database as a whole. This difference between fresh and altered rocks is partly due to the fact that the dataset to evaluate correlations within fresh samples is a hundred times larger than the datasets representing altered lithologies. The significant observation is the extremely tight correlations observed within the altered samples. For the different alteration type, Pt and Pd show the best correlation with coefficients varying between $R = 0.85$ and $R = 0.98$, whereas the weakest correlation is between Cu and Pd showing coefficients between $R = 0.24$ for the whole database and $R = 0.79$ for the epidote alteration. In conclusion, correlations between the various PGE and other metals within the intrusion are very strong in both fresh and altered rocks, locally even stronger for altered samples.

4.3. Detailed-scale remobilisation — vein study

4.3.1. pXRF analyses — element fluxes

For each sample containing a cross-cutting vein with a selvedge, the multiple results of pXRF analyses on both the altered area (selvedges of the veins) and the background area were averaged to calculate selvedge/background ratios, which are then plotted on spider-isoson diagrams (Fig. 11). The construction of these diagrams, and the rationale for using them instead of conventional isocon digrams, are discussed in the Supplementary Material.

Results are separated as a function of the vein type studied (actinolite–chlorite–epidote and quartz-carbonate veins). The elements that seem to be mostly affected by the circulation of the fluids producing the veins are K, Cu and Sr (Fig. 12), whereas Ni, S, Mn and Fe are very moderately affected. The main variations observed are summarised here:

- In the selvedge of actinolite–chlorite–epidote veins (Fig. 12a), both depletion and gain of Cu, K and Sr are observed, associated with minor variations in Zn and minor loss of Ni and S.
- The presence of thick carbonate veins is associated with small elemental fluxes, apart from loss of Ni and K for one sample (KV211-259.9).
- Finally, the presence of thin quartz-carbonate veins also seems to be associated with small variations in most elements apart from Cu and S, especially for sample KV304-157.1.

For all the samples, whatever the vein type, K and Sr show a notably heterogeneous distribution (either slightly enriched or depleted in the selvedge).

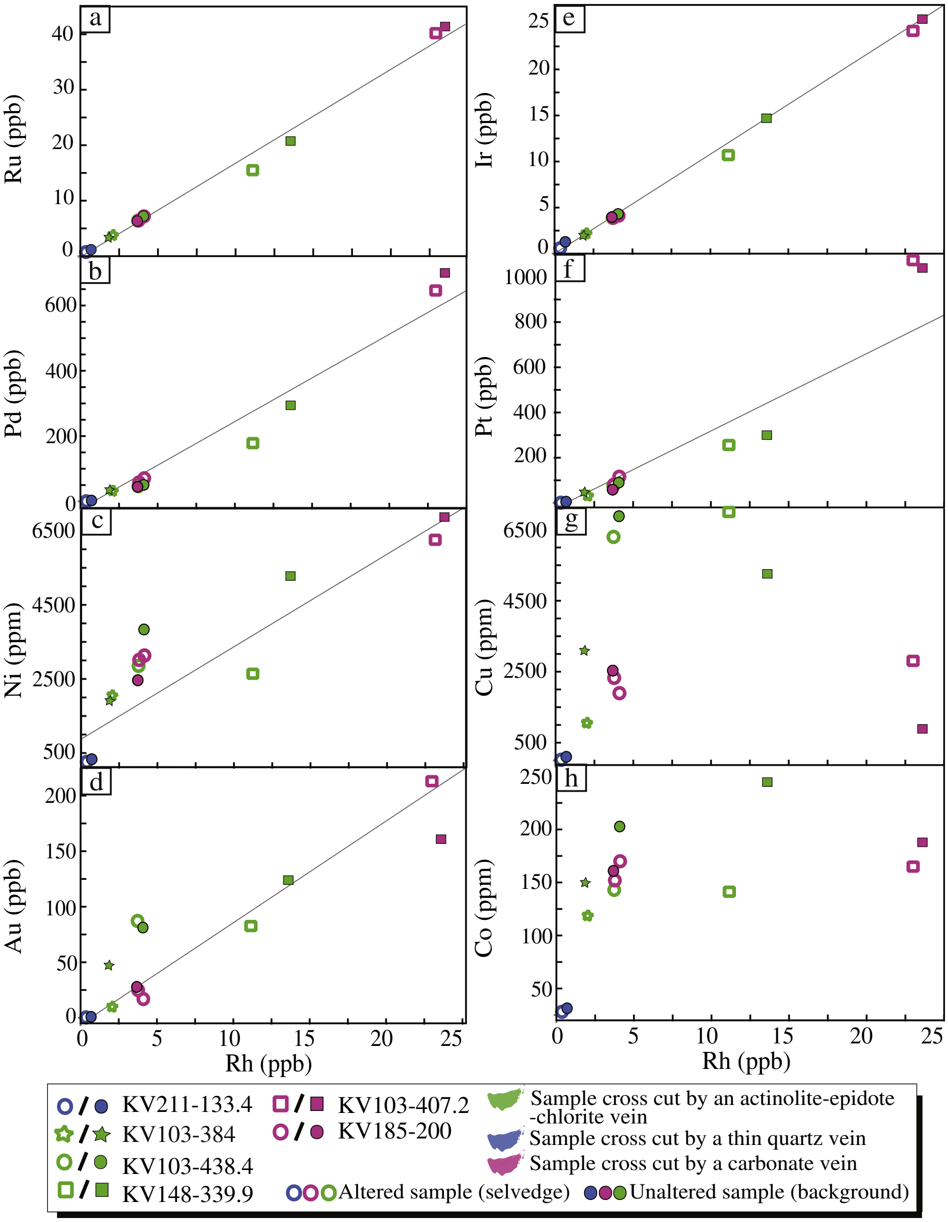

Fig. 14. Results of laboratory analyses of both altered (selvedge area) and background samples. Various chalcophile elements plotted against Rh in order to account for cm-scale heterogeneity in the modal distribution of primary sulphides.

4.3.2. Laboratory analyses — element fluxes

Results of laboratory analyses collected on a selected subset of samples from the samples previously analysed by pXRF yielded similar results and added information on the behaviour of precious metals (Fig. 13). Significant variations in K, Cu and Au concentrations are observed between the selvedge and the background areas of the various veins, and more moderate variations in Na, Mn, Ni, Co, Pd, Pt and S. Magnesium does not seem to be affected by the alteration, and similarly, no variations in concentration of IPGE (Ir, Ru and Rh) are observed (Fig. 13). When studying these spider-isocons in detail, only a few systematic associations are observed: Cu and Au are either both enriched or both depleted; Ni and Co, as well as Pd and Pt, behave similarly.

The nature of this part of the study made it necessary to collect small samples. Hence, sample precision for variations in base metals and PGE is relatively poor owing to cm-scale heterogeneity in the modal distribution of magmatic sulphides. In order to account for this heterogeneity, concentrations of all the base and precious metals were plotted against Rh, in order to visualise relative variability within the highly chalcophile elements in the sulphide fraction, rather than within the whole sample. Rhodium was chosen owing to its assumed lack of mobility during alteration coupled with its strong tendency to be concentrated in sulphide liquids rather than in platinum group minerals independent of sulphides, as can be the case for Ir, Ru and Os (Barnes and Liu, 2012; Li et al., 1996; Mungall, 2007; Mungall and Brenan, 2014). Dispersion of the more hydrothermally mobile Pt and particularly Pd should give rise to scatter around the Rh–Pt(Pd) correlation lines defined by the fresh background samples. Results show good correlations between Rh and Ru, Ir, Pd, Pt and Ni for both altered samples (selvedge) and background samples (Fig. 14). A correlation between Rh and Au still exists but is not as tight, and there is no correlation between Cu, Co and Rh (Fig. 14). These results are in agreement with observations made using the spider-isocon plots.

Finally, in order to evaluate possible decoupling between the various platinum group elements, PGE/IPGE ratios were studied and compared

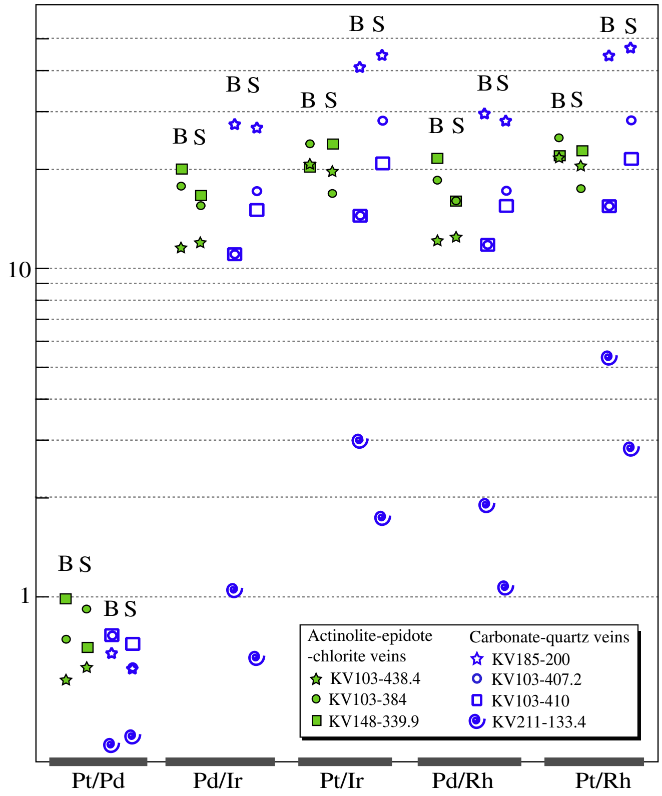

Fig. 15. Comparison of various PGE ratios between background and selvedge samples using results obtained with laboratory analyses. B = Background, S = Selvedge.

between background and selvedge samples for the two main vein types (carbonate-quartz and actinolite–chlorite–epidote) (Fig. 15). For both vein types, the Pt/Pd ratio of the selvedge compared to the background for all the different samples clusters well together. Similar results are observed for ratios of Pd and Pt against Ir and Rh.

4.3.3. Micro-XRF mapping

4.3.3.1. Elemental micro-XRF maps. Four samples were mapped using micro-XRF, and areas of particular interest were cut for thin sections. These elemental maps allow 2-D visualisation of the spatial variations in major (K, Ti, Al, Si, Ca, Mg, Mn and Fe) as well as few minor elements (Zr, Cr, Ni, Cu, S, Sr) at 25 micron spatial resolution, and permit the comparison among bulk compositions of specific sub-areas, such as vein selvedge and background, within the mapped areas. Results of these maps are shown in Figs. 16 to 18.

Combined with detailed petrographic study, these maps allow the interpretation of spatial variations in element concentrations. Selvedge-background comparisons indicate that Fe and Mn are typically depleted in the selvedge areas compared to the background areas where they are concentrated in the same mineral phase, olivine. The alteration produced by the veins within the selvedge produces a destruction of the olivine grains, first alteration to iddingsite and then complete replacement by a fine grain mixture of quartz and chlorite (cf. Petrographic study section and Fig. 6). An increase of Ca and Si in the selvedge areas is also commonly observed, which is associated with the alteration of the pyroxenes to tremolite or actinolite (cf. Petrographic study section, and Fig. 6).

Variations in the amounts of sulphides and in their composition are considered by studying 3-elemental maps (Ni, Cu and S). Apart from sample KV103-407.2 (Fig. 18), the modal proportion of sulphides does not vary much between selvedge and background areas. However, for samples KV148-438.4 and KV148-339.9, the sulphides are enriched in Cu in close proximity to the vein. Even though amounts of sulphides do not vary much in the samples, their texture differs between background and selvedge areas (as described above), associated with an enrichment in magnetite. Finally, sulphides present within the veins are mostly dominated by Cu-rich sulphides (chalcopyrite).

4.3.3.2. Element fluxes between background and selvedge areas. Areas of the micro-XRF maps were semi-quantified, and the semi-quantifications obtained were used to produce a second set of spider-isocon plots (Fig. 19). The isocons obtained show relatively flat patterns, apart from Cu that is either enriched or depleted in the selvedge. In samples KV304-305.5 (quartz vein) and KV418-339.9 (actinolite–chlorite–epidote vein), the inner selvedges are slightly depleted in Mn and Fe, and the outer selvedge slightly enriched in Mn and Fe. These variations are due to the alteration of the olivine grains to iddingsite in the outer selvedge (elevated Mn, Fe), in comparison to the absence of altered olivine replaced by a fine-grain mixture of quartz and chlorite in the inner selvedge (cf. Petrographic study, Fig. 5). A similar process is observed in sample KV304-438.4 where Cu is depleted in the inner selvedge and enriched in the outer selvedge, whereas Ni is slightly enriched in the inner selvedge and slightly depleted in the outer selvedge. Finally, Ni is also slightly depleted in the selvedge in sample KV304-305.5 and slightly enriched in the selvedge in sample KV148-339.9. But in general, all the variations that are observed are small and highly localised.

5. Discussion

5.1. Detailed-scale remobilisation — vein study

Results of the detailed-scale study of the distribution of metals and PGE, within mineralised samples that are cross cut by hydrothermal veins, indicate that Cu is the most mobile element, followed by Ni, Pd and Pt. Individual samples examined in this study show that most of the observed variations and element fluxes between the background and selvedge are minimal and only indicate cm-scale redistribution of the sulphides. In a few samples, Cu and Ni are depleted in the inner selvedge but enriched in the outer selvedge, which is interpreted as the result of cm scale reequilibration and remobilisation of the sulphides. The alteration selvedge observed around the different vein types are the result of hydration of the rock, replacing pyroxenes by amphibole and altering olivine to iddingsite. In the inner selvedge, some samples show evidence for replacement of pyrrhotite by magnetite. However, this reaction does not disrupt the relative proportions of Ni and PGE in the sulphides. Moreover, the alteration textures observed (epitaxial replacement, mm-scale variation from fresh olivine to iddingsite to clay, quartz and chlorite) are characteristic of a very low fluid-rock ratio, and this hydration does not seem to have much effect on the actual composition of the rock or on the composition and distribution of the sulphides in the sample, apart from Cu and Au concentrations, which clearly have been modified by the vein-forming processes. Platinum group elements in particular do not seem to have been affected, or in very minor proportions (Pd and Pt only), by the alteration of the samples produced by the circulation of hydrothermal fluids. Pd/Pt ratios are preserved and are very similar between background and selvedge areas of the various samples. Ratios between PPGE and IPGE such as Ir/Pt ratios are also preserved.

5.2. Deposit-scale remobilisation — database study

Results of the large scale database study indicate that hydrothermal alteration (serpentinisation, amphibolitisation and epidotisation) of the mineralised area of the Kevitsa did not affect the distribution of the platinum group elements. There is no systematic difference between the strongly correlated magmatic trends observed for the PGE between fresh pyroxenites, amphibolised pyroxenites and zones of epidote alteration. Platinum and Pd are very tightly correlated for all the different ore

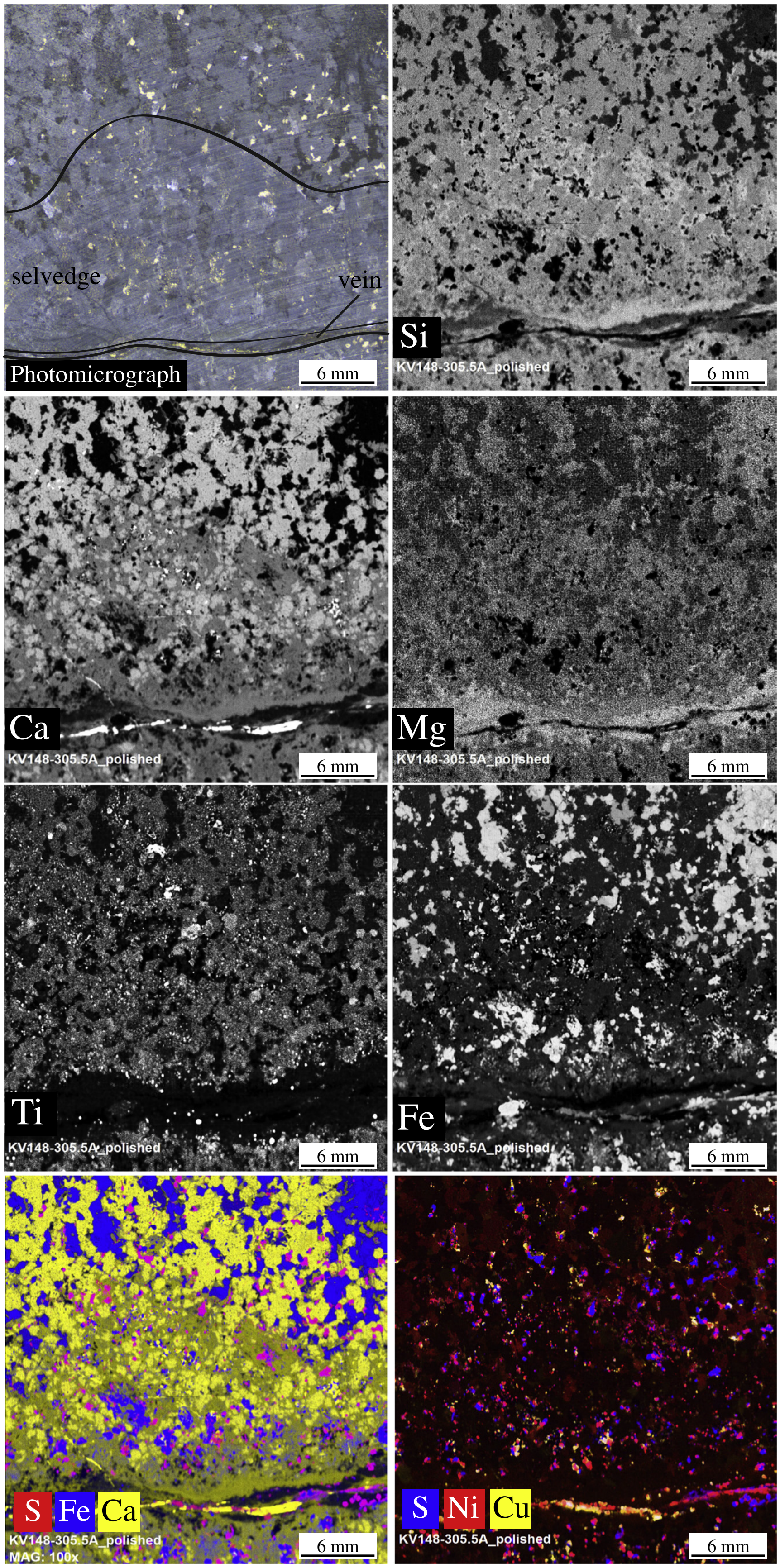

Fig. 16. Combination of representative elemental maps of sample KV148-305.5 (thin carbonate vein) obtained by micro-XRF mapping.

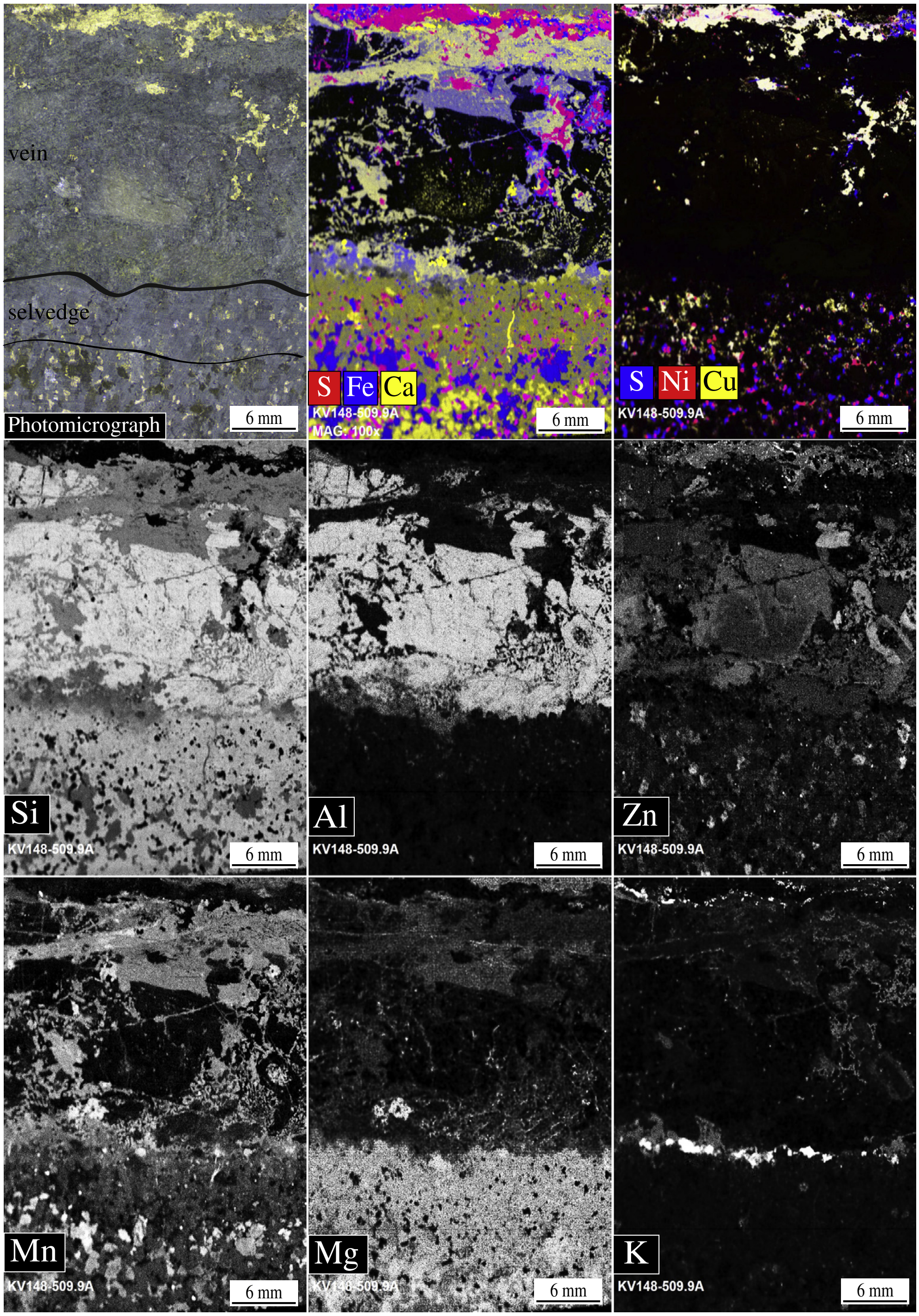

Fig. 17. Combination of representative elemental maps of sample KV148-339.9 (chlorite–albite–actinolite–epidote vein).

types and the various alterations. As Pd is more soluble than Pt under almost all conditions based on available experimental data (Barnes and Liu, 2012; Hanley, 2005; Wood, 2002), hydrothermal remobilisation would produce a decoupling between Pd and Pt concentrations, which is not observed at Kevitsa. Moreover, a very tight correlation is also observed between PPGE (Pd, Pt) and IPGE (Ir, Os, Ru and Rh). Since Pd and Pt are significantly more mobile than IPGE, an important decoupling between concentrations in Pd, Pt and IPGE would be observed if the PGE had been remobilised by hydrothermal fluids.

The only decoupling that is observed within the laboratory database is within the results obtained for samples from the Ni–PGE ore type, between Pd, Pt and IPGE. Within this ore type, Pd/Ir and Pt/Ir are significantly higher than in the other ore types (similarly for Pd/Rh, Pt/Rh) (Fig. 9). This decoupling could be attributed to the addition of Pd and Pt to the Ni–PGE ore type by hydrothermal processes. This hypothesis has been suggested before by Gervilla and Kojonen (2002). In their study, they interpret the PGE-enriched areas of the mineralisation (Ni–PGE ore) as being the results of remobilisation of PGE by chloride-rich hydrothermal fluids. These hydrothermal fluids are interpreted as chloride-rich because of the spatial association between chlorapatite and enriched Ni–PGE areas of the ore. These fluids would have been coeval with the greenschist facies metamorphism affecting the intrusion

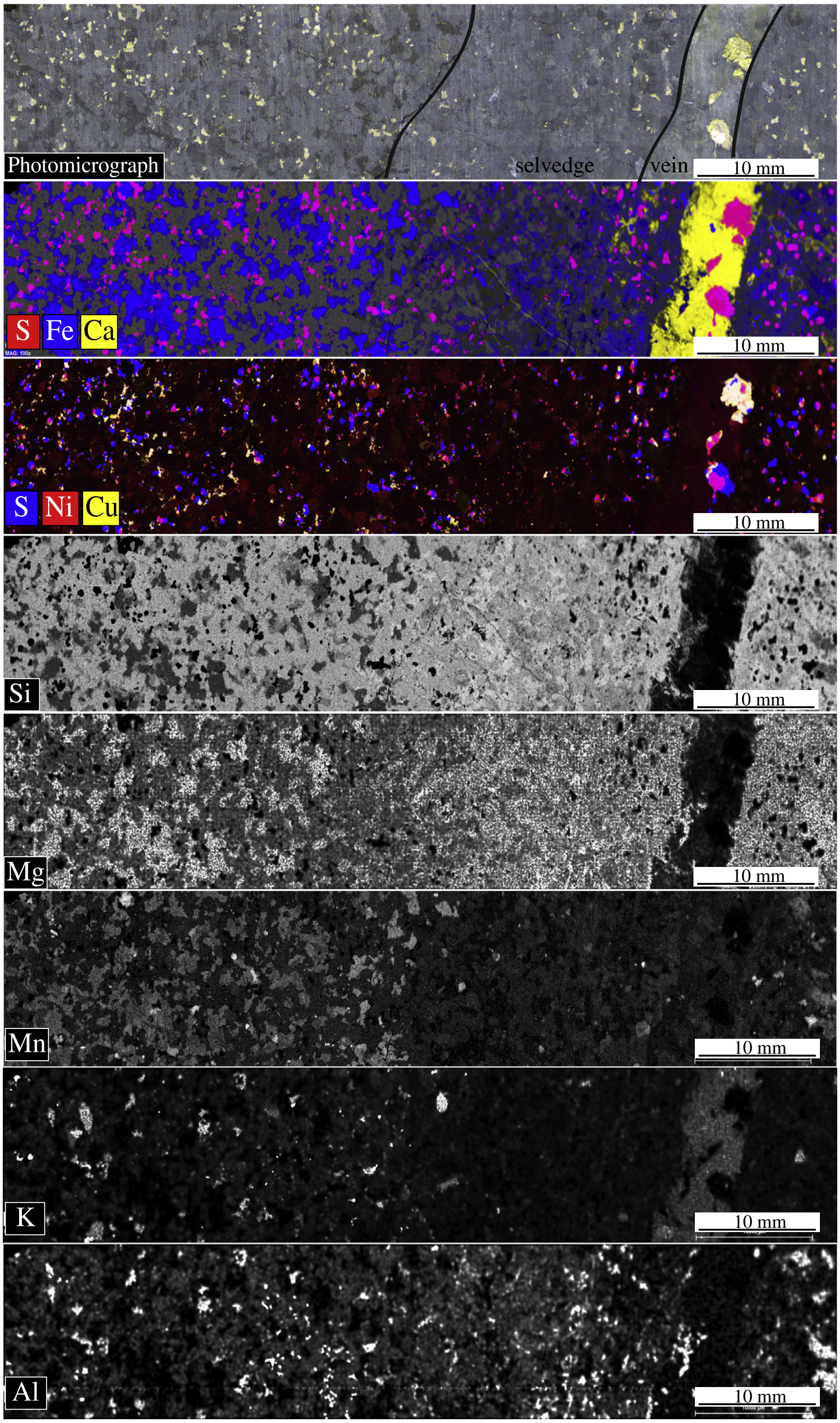

Fig. 18. Combination of representative elemental maps of sample KV103-407.2 (carbonate vein).

and could have potentially leached out PGE and As from mineralised zones and precipitated them in discrete Ni–Cu–(PGE)-rich horizons (Gervilla and Kojonen, 2002). However, this decoupling between PPGE and IPGE is not combined with decoupling between Pd and Pt, which would be expected if hydrothermal remobilisation was the cause of the decoupling, owing to the considerably higher solubility of Pd than Pt in most plausible hydrothermal solutions.

Moreover, hydrothermal enrichment in Pd, where observed in previous studies, is commonly associated with an enrichment in Cu and possibly Au. In the Kevitsa case, the Ni–PGE ore has lower concentrations in Au and Cu than the other ore types, not higher. Finally, the chlorapatite in the Kevitsa intrusion has been interpreted by Mutanen (1997) as being part of the primary intercumulus phases, rather than a later hydrothermal phase. In conclusion, the origin of

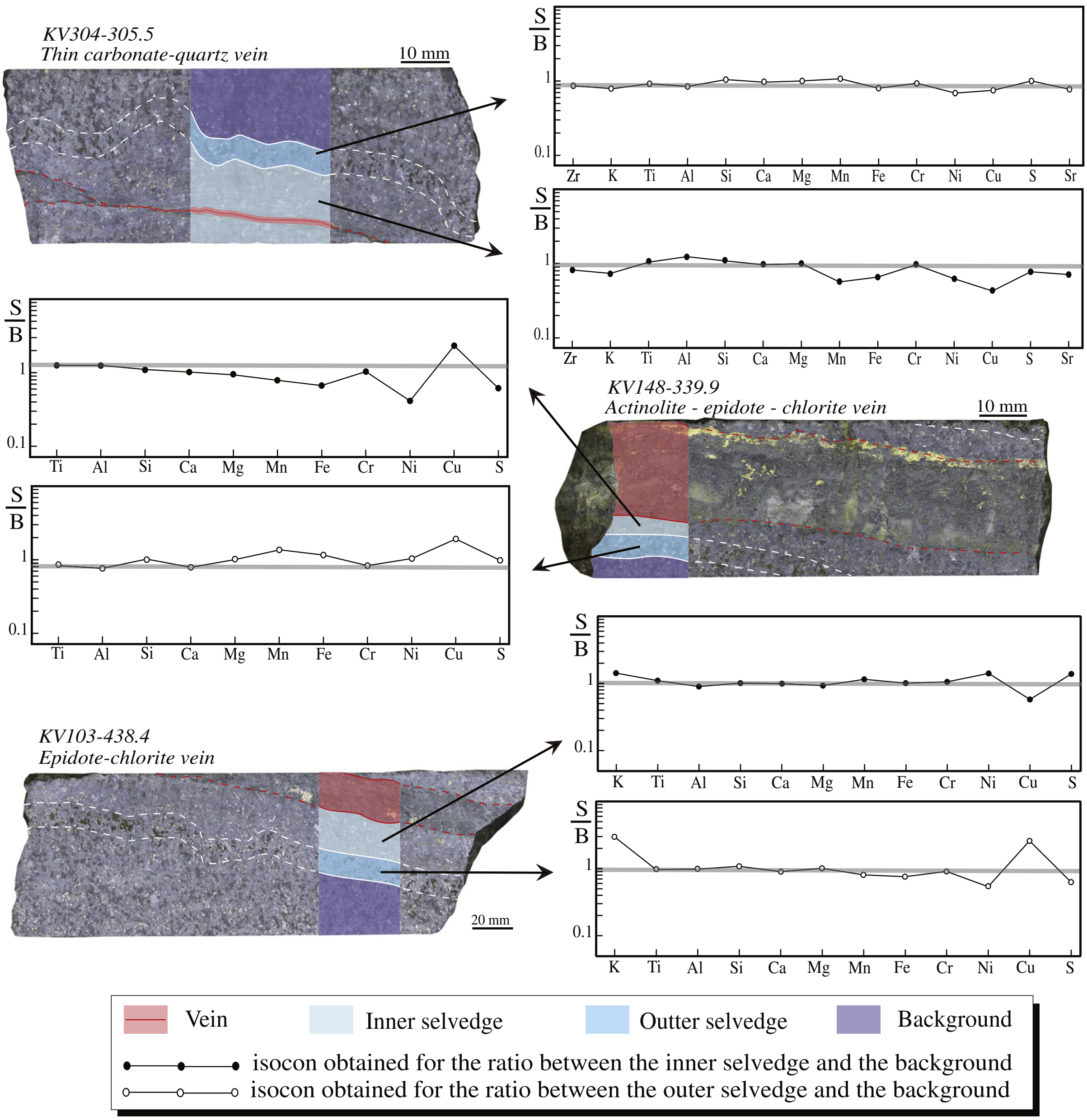

Fig. 19. Spider-isocon plots obtained by comparing the quantified composition of the background and the selvedge using quantified areas of the tornado micro-XRF maps.

the Ni–PGE ore and the decoupling between PPGE and IPGE observed within it cannot be attributed to hydrothermal processes that have so far been described.

Another interpretation for the origin of the Ni–PGE ore at Kevitsa was given by Yang et al. (2013), describing it as being the result of the assimilation of komatiite-hosted nickel-sulphides from the country rocks by the melt during emplacement. This interpretation attempts to address the extremely elevated Ni content of the olivine associated with the high Ni tenors observed within the Ni–PGE ore, suggesting a magmatic origin (pre-mineralisation). However, it does not account for the elevated Pd/Ir and Pt/Ir that are observed during the study. Indeed, the assimilation of komatiite–hosted nickel–sulphide would tend to decrease Pd/Ir, not increase it.

6. Conclusions

Combining the results of detailed-scale and mine-scale study of the distribution of metals and PGE within the Kevitsa intrusion leads to the conclusion that magmatic processes are interpreted as being the source of most of the variance observed. This study concludes that:

- low-temperature (greenschist) hydrothermal alteration did not have a significant effect on the distribution of Ni and PGE within the Kevitsa deposit, other than millimetre-scale redistribution.
- Given the important scatter, and unsystematic variability of Au and Cu within the large database, as well as the small-scale mobility observed in the vein study, Au and Cu seem to have been more mobile, and might have been redistributed by hydrothermal fluids in larger amounts and at a larger scale than Ni and PGE. It is possible that haloes of elevated Cu and Au concentration may extend into country rocks around the intrusion and may constitute a detectable hydrothermal halo, but there is no evidence of such a halo within Ni-unmineralised rocks in the intrusion itself.
- The origin of the atypical composition of the Ni–PGE remains incompletely understood but a hydrothermal origin is unlikely.

Supplementary data to this article can be found online at http://dx.doi.org/10.1016/j.oregeorev.2015.06.002.

Conflict of interest

There are no possible conflicts of interested in relation to this manuscript.

Acknowledgments

Financial support for this research was provided by MERIWA (project #M413), BHP Billiton Nickel West, Mincor Resources NL and First Quantum Minerals Ltd. This project formed part of a PhD research project at UWA, and the SIRF scholarship of the University of Western Australia and the MERIWA research grant are greatly appreciated. First Quantum Minerals Ltd (FQM) is acknowledged for providing on site access, samples and mine site assay database, especially Markku Lappaleinen who fully supported this research. The Geological Survey of Finland is also thanked for giving access to their large assay database (PGE data). This project is an output from the ARC Centre of Excellence for Core to Crust Fluid System (CCFS) and the CSIRO Mineral Resources Flagship. This is publication 630 from the ARC Centre of Excellence for Core to Crust Fluid Systems. ML Fiorentini particularly acknowledges support from the Australian Research Council through the Future Fellowship Scheme (FT110100241), ARC Linkage Grant Scheme (LP120100668), and the ARC Centre of Excellence for Core to Crust Fluid Systems. Belinda Godel, Alistair White, Steve Beresford, Eero Hanski and Harald G. Dill are thanked for their reviews of this manuscript.

References

Augé, T., Petrunov, R., Bailly, L., 2005. On the origin of the PGE mineralization in the Elatsite porphyry Cu–Au deposit, Bulgaria; comparison with the Baula–Nuasahi Complex, India, and other alkaline PGE-rich porphyries. Can. Mineral. 43, 1355–1372.

Barnes, S.J., Liu, W., 2012. Pt and Pd mobility in hydrothermal fluids: evidence from komatiites and from thermodynamic modelling. Ore Geol. Rev. 44, 49–58.

Barnes, S.J., Godel, B., Gurer, D., Brenan, J.M., Robertson, J., Paterson, D., 2013. Sulfide-olivine Fe–Ni exchange and the origin of anomalously Ni-rich magmatic sulfides. Econ. Geol. 108, 1971–1982.

Bursztyn, N.E., Olivo, G.R., 2010. PGE-rich Ni–Cu sulfide mineralization in the Flin Flon Greenstone Belt, Manitoba, Canada: implications for hydrothermal remobilization of platinum group elements in basic–ultrabasic sequences. Econ. Geol. 105, 1469–1490.

Capistrant, P.L., Hitzman, M.W., Wood, D., Kelly, N.M., Williams, G., Zimba, M., et al., 2015. Geology of the enterprise hydrothermal nickel deposit, North-Western Province, Zambia. Econ. Geol. 110, 9–38.

Coppard, J., Klatt, S., Ihlenfeld, C., 2013. The Sakatti Ni–Cu–PGE deposit in northern Finland. In: Hanski, E., Maier, W. (Eds.), Excursion Guidebook FINRUS, Ni–Cr–PGE Deposits of Finland and the Kola Peninsula. 12th SGA Biennial Meeting, Mineral Deposit Research for a High-tech World, Geological Survey of Sweden, Uppsala, Sweden, pp. 10–11.

De Almeida, C.M., Olivo, G.R., de-Carvalho, S.G., 2007. The Ni–Cu–PGE sulfide ores of the komatiite-hosted Fortaleza de Minas deposit, Brazil: evidence of hydrothermal remobilization. Can. Mineral. 45, 751–773.

Dillon-Leitch, H.C.H., Watkinson, D.H., Coats, C.J.A., 1986. Distribution of platinum-group elements in the Donaldson West Deposit, Cape Smith Belt, Quebec. Econ. Geol. 81, 1147–1158.

Economou-Eliopoulos, M., 1991. Platinum-group element and gold contents in the Skouries porphyry copper deposit, Chalkidiki Peninsula, northern Greece. Econ. Geol. 86, 740–749.

Farrow, C.E.G., Watkinson, D.H., 1997. Diversity of precious-metal mineralization in footwall Cu–Ni–PGE deposits, Sudbury, Ontario: implications for hydrothermal models of formation. Can. Mineral. 35, 817–839.

Gal, B., Molnár, F., Peterson, D.M., 2011. Cu–Ni–PGE mineralization in the South Filson Creek area, South Kawishiwi Intrusion, Duluth Complex; mineralization styles and magmatic and hydrothermal processes. Econ. Geol. 106, 481–509.

Gammons, C.H., 1995. Experimental investigations of the hydrothermal geochemistry of platinum and palladium: IV. The stoichiometry of Pt(IV) and Pd(II) chloride complexes at 100 to 300 °C. Geochim. Cosmochim. Acta 59, 1655–1667.

Gammons, C.H., 1996. Experimental investigations of the hydrothermal geochemistry of platinum and palladium: V. Equilibria between platinum metal, Pt(II), and Pt(IV) chloride complexes at 25 to 300 °C. Geochim. Cosmochim. Acta 60, 1683–1694.

Gervilla, F., Kojonen, K., 2002. The platinum-group minerals in the upper section of the Keivitsansarvi Ni–Cu–PGE deposit, Northern Finland. Can. Mineral. 40, 377–394.

González-Álvarez, I., Sweetapple, M., Lindley, I.D., Kirakar, J., 2013. Hydrothermal Ni: Doriri Creek, Papua New Guinea. Ore Geol. Rev. 52, 37–57.

Grant, J.A., 1986. The isocon diagram; a simple solution to Gresens' equation for metasomatic alteration. Econ. Geol. 81, 1976–1982.

Gregory, J., 2011. SEDAR Report. First Quantum Minerals LTD, p. 364.

Gresens, R.L., 1967. Composition–volume relationships of metasomatism. Chem. Geol. 2, 47–65.

Gresham, J.J., 1986. Depositional environments of volcanic peridotite-associated nickel deposits with special reference to the Kambalda dome. In: Genkin, G.H., Naldrett, A., Ridge, A.J., Sillitoe, R.H., Vokes, F.M. (Eds.), Twenty-Seventh International Geological Congress-Moscow. Springer-Verlag, Berlin, pp. 63–90.

Grinenko, L.N., Hanski, E., Grinenko, V.A., 2003. Formation conditions of the Keivitsa Cu–Ni deposit, Northern Finland: evidence from S and C isotopes. Geochem. Int. 41, 154–167.

Hanley, J., 2005. The aqueous geochemistry of the platinum-group elements (PGE) in surficial, low-T hydrothermal and high-T magmatic hydrothermal environments. In: Mungall, J.E. (Ed.), Exploration for Platinum-Group Element Deposits, Mineralogical Association of Canada Short Course Series, pp. 35–56.

Hanley, J.J., Mungall, J.E., 2003. Chlorine enrichment and hydrous alteration of the Sudbury Breccia hosting footwall Cu–Ni–PGE mineralization at the Fraser mine, Sudbury, Ontario, Canada. Can. Mineral. 41, 857–881.

Hanski, E., Huhma, H., 2005. Central Lapland greenstone belt. In: Lehtinen, M., Nurmi, P.A., Rämö, T.O. (Eds.), Precambrien Geology of Finland — Key to the Evolution of the Fennoscandian Shield. Elsevier, Amsterdam, pp. 139–194.

Hanski, E., Huhma, H., Rastas, P., Kamenetsky, V.S., 2001. The paleoproterozoic komatiite–picrite associations of Finnish Lapland. J. Petrol. 42, 855–876.

Heath, C., Lahaye, Y., Stone, W.E., Lambert, D., 2001. Origin of variations in nickel tenor along the strike of the Edwards lode nickel sulfide orebody, Kambalda, Western Australia. Can. Mineral. 39, 655–671.

Heggie, G.J., Barnes, S.J., Fiorentini, M., 2013. Application of lithogeochemistry in the assessment of nickel-sulphide potential in komatiite belts from northern Finland and Norway. Bull. Geol. Soc. Finl. 85, 107–126.

Jaireth, S., 1992. The calculated solubility of platinum and gold in oxygen-saturated fluids and the genesis of platinum–palladium and gold mineralization in the unconformity-related uranium deposits. Mineral. Deposita 27, 42–54.

Keays, R.R., Jowitt, S.M., 2013. The Avebury Ni deposit, Tasmania: a case study of an unconventional nickel deposit. Ore Geol. Rev. 52, 4–17.

Le Vaillant, M., Barnes, S.J., Fisher, L., Fiorentini, M.L., Caruso, S., 2014. Use and calibration of portable X-ray fluorescence analysers: application to lithogeochemical exploration for komatiite-hosted nickel sulphide deposits. Geochem. Explor. Environ. Anal. 14, 199–209.

LeFort, D., Hanley, J.J., Guillong, M., 2011. Subepithermal Au–Pd mineralization associated with an alkalic porphyry Cu–Au deposit, Mount Milligan, Quesnel Terrane, British Columbia, Canada. Econ. Geol. 106, 781–808.

Lehtonen, M., Airo, M.L., Eilu, P., Hanski, E., Kortelainen, V., Lanne, E., et al., 1998. The stratigraphy, petrology and geochemistry of the Kittilä greenstone area, northern Finland. Report Invest, Geological Survey of Finlandpp. 140–144.

Lesher, C.M., Keays, R.R., 1984. Metamorphically and hydrothermally mobilized Fe–Ni–Cu sulphides at Kambalda, Western Australia. In: Buchanan, D.L., Jones, M.J. (Eds.), Sulphide Deposits in Mafic and Ultramafic Rocks. Institute of Mineralogy and Metallogeny, London, pp. 62–69.

Li, C., Barnes, S.J., Makovicky, E., Rose, Hansen J., Makovicky, M., 1996. Partitioning of nickel, copper, iridium, rhenium, platinum, and palladium between monosulfide solid solution and sulfide liquid: effects of composition and temperature. Geochim. Cosmochim. Acta 60, 1231–1238.

Liu, W., Migdisov, A., Williams-Jones, A., 2012. The stability of aqueous nickel(II) chloride complexes in hydrothermal solutions: results of UV–visible spectroscopic experiments. Geochim. Cosmochim. Acta 94, 276–290.

Mei, Y., Etschmann, B., Liu, W., Sherman, D.M., Barnes, S.J., Fiorentini, M.L., Seward, T.M., Testemale, D., Brugger, J., 2015. Palladium complexation in chloride— and bisulfide—rich fluids. Insights from ab initio molecular dynamics simulations and X—ray absorption spectroscopy: Geochimica et Cosmochimica Acta 161, 128–145.

Mernagh, T.P., Heinrich, C.A., Leckie, J.F., Carville, D.P., Gilbert, D.J., Valenta, R.K., et al., 1994. Chemistry of low-temperature hydrothermal gold, platinum, and palladium (+ or − uranium) mineralization at Coronation Hill, Northern Territory, Australia. Econ. Geol. 89, 1053–1073.

Molnár, F., Watkinson, D.H., 2001. Fluid-inclusion data for vein-type Cu–Ni–PGE footwall ores, Sudbury Igneous Complex and their use in establishing an exploration model for hydrothermal PGE-enrichment around mafic–ultramafic intrusions. Explor. Min. Geol. 10.

Molnár, F., Watkinson, D., Jones, M.J., 2001a. Multiple hydrothermal processes in footwall units of the North Range, Sudbury Igneous Complex, Canada, and implications for the genesis of vein-type Cu–Ni–PGE deposits. Econ. Geol. 96, 1645–4670.

Molnár, F., Watkinson, D.H., Jones, P.C., 2001b. Multiple hydrothermal processes in footwall units of the North Range, Sudbury Igneous Complex, Canada, and implications for the genesis of vein-type Cu–Ni–PGE deposits. Econ. Geol. 96, 1645–1670.

Mountain, B., Wood, S., 1988. Solubility and transport of platinum-group elements in hydrothermal solutions: thermodynamic and physical chemical constraints. In: Prichard, H.M., Potts, P.J., Bowles, J.F.W., Cribb, S.J. (Eds.), Geo-Platinum 87. Springer, Netherlands, pp. 57–82.

Mungall, J.E., 2007. Magmatic ore deposits. In: Rudnick, R. (Ed.), The Crust Treatise on Geochemistry. Pergamon, Oxford, pp. 1–31.

Mungall, J.E., Brenan, J.M., 2014. Partitioning of platinum-group elements and Au between sulfide liquid and basalt and the origins of mantle–crust fractionation of the chalcophile elements. Geochim. Cosmochim. Acta 125, 265–289.

Mutanen, T., 1997. Geology and Ore Petrology of the Akanvaara and Koitelainen Mafic Layered Intrusions and the Keivitsa–Satovaara Layered Complex, northern Finland. Geological Survey of Finland.

Mutanen, T., Huhma, H., 2001. U–Pb geochronology of the Koitelainen, Akanvaara and Keivitsa layered intrusions and related rocks. In: Vaasjoki, M. (Ed.), Radiomatric Age Determinations from Finnish Lapland and Their Bearing on the Timing of Precambrian Volcano-Sedimentary Sequences. Geological Survey of Finland, pp. 229–246.

Pirajno, F., González-Álvarez, I., 2013. A re-appraisal of the Epoch nickel sulphide deposit, Filabusi Greenstone Belt, Zimbabwe: a hydrothermal nickel mineral system? Ore Geol. Rev. 52, 58–65.

Santaguida, F., Luolavirta, K., Lappalainen, M., Ylinen, J., Voipio, T., Jones, S., 2015. Chapter 3.6 - The Kevitsa Ni-Cu-PGE Deposit in the Central Lapland Greenstone Belt in Finland. In: O'Brien, W.D.M.L. (Ed.), Mineral Deposits of Finland. Elsevier, pp. 195–210.

Schiffries, C.M., 1976. The petrogenesis of a platiniferous dunite pipe in the Bushveld Complex: infiltration metasomatism by a chloride solution. Econ. Geol. 71, 249–260.

Standing, J., De Luca, K., Outhwaite, M., Neilson, I., Lappalainen, M., Wijns, C., et al., 2009. Report and Recommendations from the Kevitsa Campaign. Jigsaw Geoscience Pty Ltd, Finland.

Wang, C.Y., Prichard, H.M., Zhou, M.-F., Fisher, P.C., 2008. Platinum-group minerals from the Jinbaoshan Pd–Pt deposit, SW China: evidence for magmatic origin and hydrothermal alteration. Mineral. Deposita 43, 791–803.

Wood, S.A., 2002. The aqueous geochemistry of the platinum-group elements with applications to ore deposits. In: Cabri, L.J. (Ed.), The Geology, Geochemistry, Mineralogy and Mineral Beneficiation of Platinum-Group Elements. Canadian Institute of Mining and Metallurgy, pp. 211–249.

Yang, S.-H., Maier, W., Hanski, E., Lappalainen, M., Santaguida, F., Määttä, S., 2013. Origin of ultra-nickeliferous olivine in the Kevitsa Ni–Cu–PGE-mineralized intrusion, northern Finland. Contrib. Mineral. Petrol. 166, 81–95.